

Characteristics of source and reservoir rocks of the Eocene Mangahewa Formation in Taranaki Basin, New Zealand: their implications for petroleum systems

Mohamed R. Shalaby^{1,2,*}, Nurhazwana Jumat¹, Md. Aminul Islam¹ and Stavros Kalaitzidis³

¹Geosciences, Faculty of Science, Universiti Brunei Darussalam,
Jalan Tungku Link, BE 1410, Brunei Darussalam

²Geology Department, Faculty of Science, Tanta University, Tanta 31527, Egypt

³Department of Geology, University of Patras, GR-26504 Rio-Patras, Greece

*corresponding author email: mshalaby2004@yahoo.com

Abstract

The Middle to Late Eocene Mangahewa Formation in the Taranaki Basin has been evaluated for its petroleum system (source potential and reservoir qualities). The Mangahewa Formation is generally interpreted as an alternating margin to shallow marine environment, with lithologies consisting of sandstone, siltstone, mudstone, and bituminous coal. The Rock-Eval pyrolysis results show very good source rock generative potential with a total organic carbon content of 0.8-90.02 wt. % and hydrogen index values in the range of 54-491 mg HC/g TOC, with a predominance of oil- and/or gas-prone, mixed Type II-III kerogen. Organic petrographical data reveal that the coals are rich in perhydrous vitrinite, whereas the shales are rich in alginite and bituminite, displaying frequent migrabitumens. Biomarker analysis suggests a predominantly terrigenous origin, whereas the pyrolysis T_{max} data (414–447°C) and other maturity indicators such as biomarkers and vitrinite reflectance show immature and mature samples. Petrographic analyses using optical microscopy and SEM of the reservoir sandstone samples show that the occurrence of compaction and cementation is succeeded by the leaching of feldspars and dissolution of calcite cement. The reservoir samples on the whole exhibit good reservoir quality, with an average porosity of 15.7%, an average permeability of 1678.9mD and an average water saturation of 21.4%. The source and reservoir units are part of a complete petroleum system of the Mangahewa Formation, with the overlying Turi Formation as the seal rock. The petroleum processes of maturation, generation and migration, which started in the Lower Miocene (18.8 Ma), have been recorded in many stratigraphic traps within the Mangahewa Formation and in other faulted structural traps due to migration. The generation process is expected to be continuing in the present day as the source approaches maturity, and it has not yet reached peak generation.

Index Terms: source and reservoir rocks, Rock-Eval pyrolysis, biomarkers, Mangahewa Formation, Taranaki Basin, petroleum systems

1. Introduction

The Taranaki Basin is considered to be the most productive sedimentary basin in New Zealand. It is located mainly offshore on the west coast of New Zealand (see *Figure 1*), with an areal extent of 100,000 km². The petroleum generation of the sole prolific basin of New Zealand has been studied by many researchers.¹ In the Taranaki

Basin, the hydrocarbons are sourced from the carbonaceous formations of the Late Cretaceous to the Paleocene, and petroleum has been discovered throughout its stratigraphic record, with the most productive reservoirs in the Paleogene age.¹

The variable lithological content of the Middle to Late Mangahewa Formation contributes to the potential of the formation, which is both a high-quality source and a high-quality reservoir. Study of the source rock characteristics is of great importance for understanding the different types of organic matter, level of maturity, migration pathways and mechanisms, and productivity of an oil-field.² The organic richness, volume and maturity of a source rock are essential parameters in determining its hydrocarbon potential. Parameters like the type of organic matter, depositional paleoenvironments, and burial history are also very important.^{2,3}

Many studies have been conducted on the source rocks of the Taranaki Basin,⁴⁻⁹ including in particular the Mangahewa source rock.^{10,11} Jumat¹² included the Mangahewa Formation as part of a source rock integrated study, combining geochemical and well logging data on several source rocks in the Taranaki Basin. Many studies have previously been made of source rocks in different oil basins all over the world.¹³⁻²⁴

In this study, the Mangahewa Formation is assessed for its oil generation potential, using organic geochemical analyses and petrographical examination. The methodological approach includes the determination of the total organic carbon (TOC) content, Rock-Eval pyrolysis, organic petrography, vitrinite reflectance measurements, and geochemical biomarkers.

An effective source rock will be unproductive unless it is successfully contained by a good reservoir interval, typically overlying the source. A good reservoir fundamentally possesses good porosity and permeability, so as to store hydrocarbons that have migrated from the source in quantities sufficient for commercial drilling.

Some studies of the characteristics and quality evolution of other reservoirs in the Taranaki Basin have previously been made, such as the Farewell Formation²⁵, the McKee Formation²⁶ and many other fields.²⁷⁻²⁹

In this research paper, the reservoir quality of the Mangahewa Formation is studied via the integration of different datasets, which include core analyses, petrographic descriptions and well log data.

In general, many separate publications are available on source rock or reservoir characterization, but no such integrated study has been made before for the Mangahewa Formation. This paper aims to analyze and evaluate the availability of the petroleum system of the Middle to Late Mangahewa Formation in the Taranaki Basin, New Zealand. The types of organic matter and the richness and associated oil generation potential of the source rock samples are discussed, as are the reservoir quality evolution and the petrophysical characteristics of the Mangahewa Formation. Moreover, the paper includes a brief discussion of the subsurface structural configuration and trapping mechanism.

The ultimate aim of the paper is to achieve a comprehensive study of the petroleum system of the Mangahewa Formation that takes into account its source and reservoir characterization. This is done using a suite of data, taken from Rock-Eval pyrolysis, organic petrology, geochemical biomarkers, petrographic and petrophysical examinations, and well logs.

2. Geological background of the Taranaki Basin

The Taranaki Basin remains the only commercially producing basin in New Zealand, with the largest hydrocarbon reserves. It is located predominantly offshore, with the onshore area mostly within the Taranaki Peninsula. Numerous studies have covered the geological evolution of Taranaki Basin.³⁰⁻³⁵ The Taranaki Basin was formed as a result of the breakup of the supercontinent Gondwana, which split Australia and Zealandia. The Tasman Sea, along with a number of extensional basins on the New Zealand subcontinent, was produced as a result, including an intra-plate rift that created the Taranaki Rift. This rift would later become the Taranaki Basin during the Late Cretaceous.^{30,36,37}

The basin evolved in three phases: (1) A rifting stage during the mid-Cretaceous to Paleocene, when coal deposition occurred in restricted, fault-controlled basins; (2) A passive margin, formed by thermal contraction and regional subsidence during the Eocene to Early Oligocene, when coal deposition occurred in transgressive coastal plains and marginal marine settings; and (3) An active marginal marine during the Oligocene to Recent, resulting from the convergence of the Australia-Pacific plate boundary through what is now New Zealand.³¹

Two main structural blocks have been generated in the Taranaki Basin: (1) the Western Stable Platform and (2) the Eastern Mobile Belt^{32,35,38} (see **Figure 1**). The offshore western part of the basin corresponds to the Western Stable Platform and was affected by late Cretaceous to Eocene normal block faulting. By contrast, the Eastern Mobile Belt experienced numerous tectonic processes and its evolution involved uplifting with normal, reverse, and overthrust faulting.³¹

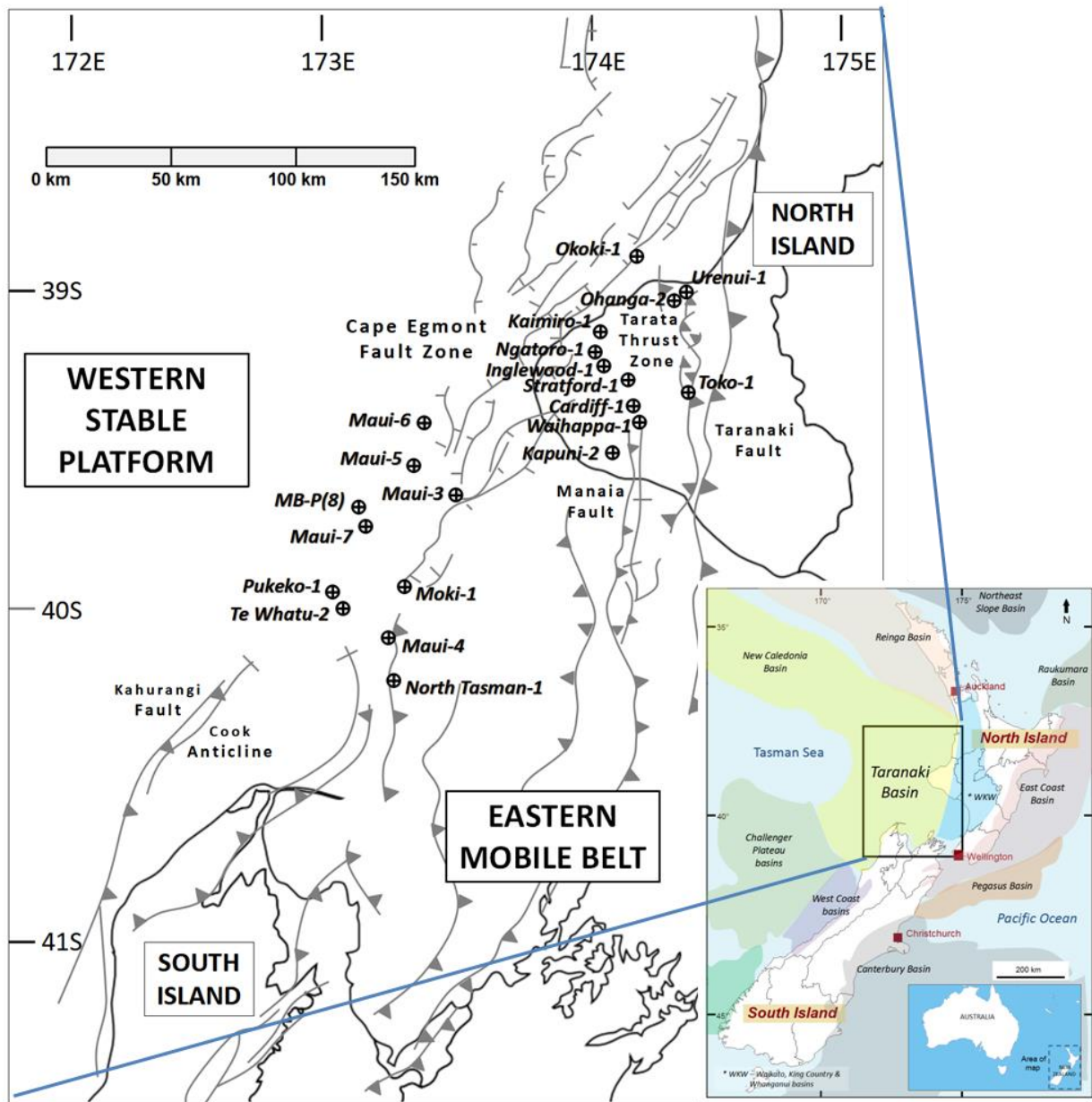


Figure 1. Map showing the Taranaki Basin in New Zealand and the distribution of the wells under study.^{1,23}

The generalized stratigraphy of the Taranaki Basin is made up of terrigenous and marine sedimentary and volcanic rocks of the Late Cretaceous to recent (see **Figure 2**). The basin contains predominantly marine strata, with significant terrestrial sedimentation occurring between the Middle Cretaceous and Eocene. The succession has been classified into four megasequences:³¹

(1) An Upper Cretaceous syn-rift sequence (the Pakawau Group)

- (2) A Paleocene to Eocene late-rift and post-rift transgressive sequence (the Kapuni and Moa groups)
- (3) An Oligocene to Miocene foredeep and distal sediment starved shelf and slope sequence (the Ngatoro Group) and a Miocene regressive sequence (the Wai-iti Group)
- (4) A Plio-Pleistocene regressive sequence (the Rotokare Group)

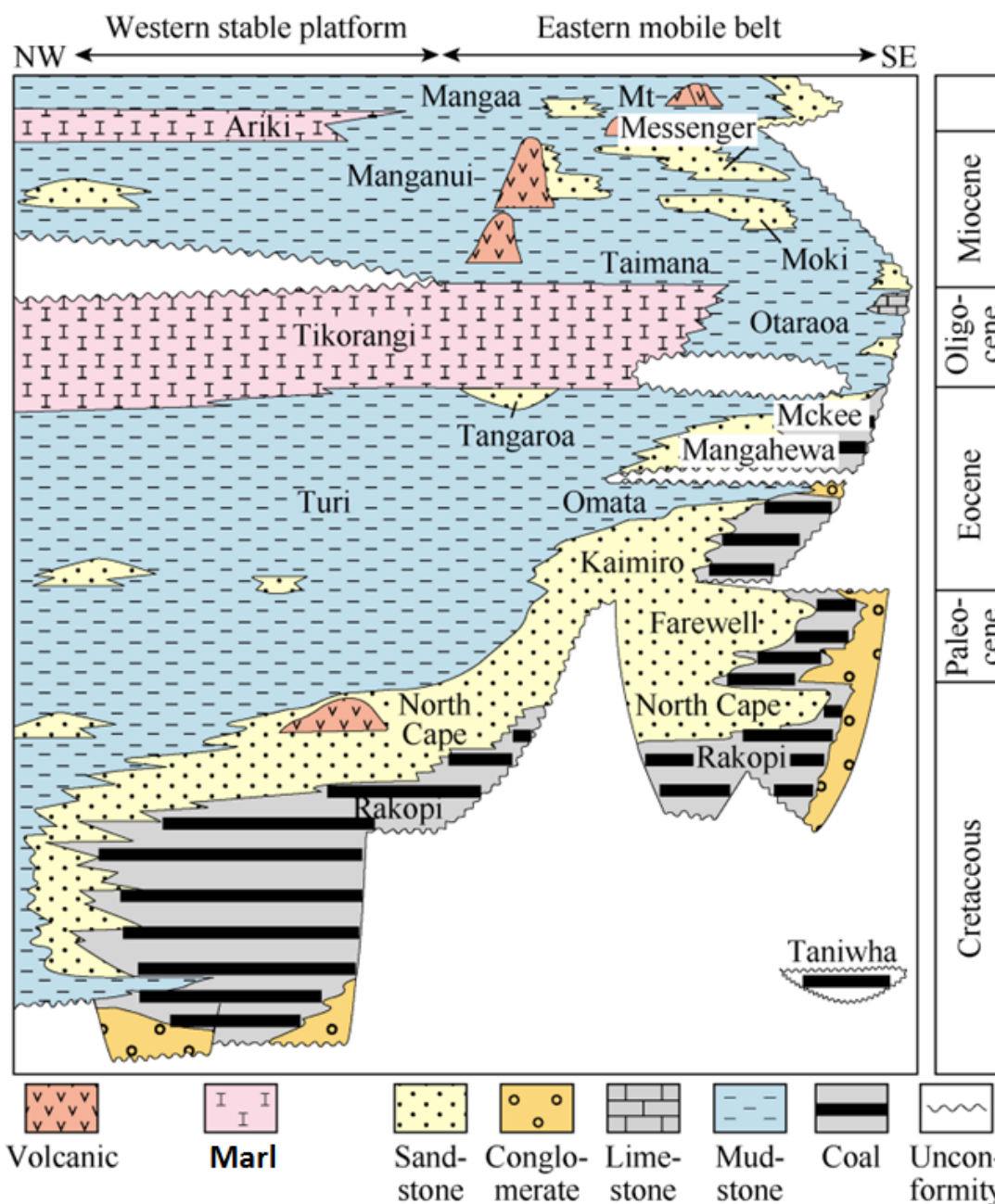


Figure 2. The generalized chronostratigraphy succession, from Cretaceous to Cenozoic, of the Taranaki Basin.^{1,23}

The Mangahewa Formation is part of the Kapuni Group, which alongside the Moa Group, was formed as part of the transgressive sequence resulting from the regional post-rift subsidence. The Kapuni Group encompasses three other formations: the oldest Farewell Formation, the Kaimiro Formation, and the youngest McKee Formation. The Moa Group is the marine equivalent and is made up of marine mudstones of the Turi and Tangaroa formations. The Turi Formation inter-fingers with other formations from the Kapuni Group. As transgression continued through the Eocene, there was an increase in the sedimentation of the Moa Group and, subsequently, there was a decline in the deposition of the Kapuni Group. By the end of the Eocene, the Taranaki Group was eventually covered by fine-grained, terrigenous sediments of the Moa Group.

Alternative episodes of transgression and regression resulted in the deposition of the Mangahewa Formation in marine, marginal marine, shallow marine and terrestrial systems. The Mangahewa Formation consists mostly of sandstone, siltstone, mudstone, and bituminous coal. Its variable lithology contributes to it being both a good potential source and a high-quality reservoir. The Mangahewa Formation source rocks have been found to have very good generation potential, with oil-prone Type-II, oil-and/or gas-prone Type-II/III, and gas condensate Type-III kerogen.¹¹ This study improves upon the previous study by the addition of organic petrography and reservoir assessment.

3. Methodology

The dataset and samples used in this paper have been obtained with permission for re-evaluation and publication from the New Zealand Ministry of Business, Innovation, and Employment (MBIE). The rock samples were collected from the National Core House, Wellington, New Zealand during September-October 2016.

The Mangahewa Formation dataset used in this study for source rock characterization includes Rock-Eval pyrolysis data (88 samples), organic

petrography and vitrinite reflectance data (37 samples), and biomarker data, represented here by 46 analyzed samples. The dataset for reservoir rock characterization are represented in this study by the petrophysical parameters measured for 16 core samples, petrography data (12 thin sections prepared from rock samples collected from the Maui-5, Maui-6 and Maui-7 wells, from which some samples have been used for SEM analyses as well), well log data and well completion reports from 22 wells scattered across the basin. The locations of these wells are shown in **Figure 1**.

3.1 Source rock characterization

The Rock-Eval pyrolysis data (S_1 , S_2 , S_3 , T_{max} , and TOC) and the calculated parameters (HI, OI and PI) for the Mangahewa Formation samples have been listed in **Table 1**. The data used were taken from 15 wells, as shown in **Figure 1** (Cardiff-1, Kapuni-2, Kaimiro-1, Inglewood-1, Maui-4, Maui-5, Maui-6, Ngatoro-1, North Tasman-1, Ohanga-2, Okoki-1, Pukeko-1, Urenui-1, Waihappa-1, and Waihappa-1A).

The organic petrographical data, including the maceral analysis and vitrinite reflectance measurements of the coal samples, were obtained from the MBIE dataset. Additional shale samples from the Maui-5 and Maui-6 wells were examined at the University of Patras, Greece. This analysis was applied only to some of the shale samples selected from the Maui-5 and Maui-6 wells, due to the unavailability of coal and shaly coal rock samples. The polished blocks were prepared from crushed samples ($\varnothing < 1$ mm) according to International Standards³⁹ and examined under oil immersion using a LEICA DMRX microscope⁴⁰, and the nomenclature of the ICCP System for the macerals⁴¹⁻⁴⁴ and the solid bitumen.⁴⁵ The reflectance measurements were taken using the standard procedure for dispersed organic matter.⁴⁰ The reflectance measurements obtained for the solid bitumens were converted to equivalent vitrinite reflectance values⁴⁶ (VR%), for use as a thermal maturity indicator (see **Table 2**). It should be noted that the organic petrographical results presented here are only for the shale samples, which are not

representative of the coal and shaly coal lithologies present in the Mangahewa Formation. A quantitative analysis of the maceral composition of the coal and shaly coal samples, obtained from the MBIE dataset, is listed in **Table 3**.

Tables 4, 5 and 6 list the biomarker characteristics of the selected samples. The dataset comprises GC-MS results for n-alkanes and isoprenoids, hopanes and terpanes, and steranes. The dataset was selected from six wells (Kaimiro-1, Maui-4, Ohanga-2, Okoki-1, Waihapa-1, and Waihapa-1A).

3.2 Reservoir rock characterization

The Maui-5, Maui-6, Maui-7, MB-P(8), and Moki-1 wells were selected for reservoir characterization (see **Figure 1**). An integrated reservoir rock characterization was made using a combination of petrophysical analysis, sedimentological and petrographic studies, and well-log interpretation.

A reservoir quality investigation was carried out through analyses of the principal petrophysical parameters of porosity and permeability. Two data points from both the Maui-5 and MB-P(8) wells, 3 data points from the Maui-6 well, and 9 data points from the Moki-1 well were assessed (see **Table 7**). A statistical analysis was performed, and the petrophysical parameters used to determine whether the formation has promising reservoir quality, based on the standard classification.⁴⁷

The petrography data consists of two datasets: photomicrographs for the Maui-5, Maui-6, and Maui-7 wells provided by MBIE, and core samples from the same wells which were used to prepare new thin sections in the laboratory at Universiti Brunei Darussalam (UBD). The thin sections were prepared by vacuum impregnation with blue-eyed resin before being cut and ground to a standard 30 μm thickness. The blue-eyed resin helps to distinguish the porosity types. The thin sections were examined using a standard Zeiss polarizing microscope. The sedimentological features of the Mangahewa

Formation have been examined, including the pore spaces and the diagenetic attributes of compaction, cementation, dissolution, and recrystallization.

In addition, a scanning electron microscope (SEM) analysis was applied to selected core samples from three wells (Maui-5, Maui-6, and Maui-7) to identify features not visible under the polarizing microscope/photomicrographs, and hence to further support the findings of the earlier petrography dataset. The samples were coated with carbon and platinum before the analysis, which was performed with an accelerating voltage of 10 kV to 20 kV and a beam current of 90 μA to 30 nA.

Interactive Petrophysics (IP) software was used to carry out log-based petrophysical analyses of the aforementioned wells in the Mangahewa Formation. The formation is found in the sections at 2804-3075 m (80 m thick) for the Maui-5 well, at 2785-3002 m (217 m thick) for the Maui-6 well, 2695-2990 m (295 m thick) for Maui-6 well, and at 2073-2410 m (337 m thick) for the Moki-1 well. The log data includes conventional measurements, such as resistivity logs (a microspherical focused log, deep lateral log, and deep induction log), and neutron, density, sonic, and gamma ray logs.

The PetroMod software developed by Schlumberger was used to generate a one-dimensional model, for the analysis of the burial and thermal maturity histories of the Mangahewa Formation in the Cardiff-1 Well. The input data for the model includes the names, top, bottom, and thickness of the formations penetrated by the well, the formation age (in Ma), the measured borehole temperature (in Celsius), and the measured vitrinite reflectance (% R_o). A constant heat flow of 60 mW/m^2 and a kinetic model type T_II were selected.^{48,49} The latter was chosen because of its suitability for terrigenous, non-marine, and waxy source rocks, such as comprise the Mangahewa Formation. The bottom hole temperature values were corrected prior to model calibration, because the bottom hole temperature is typically measured before the formation and

drilling mud temperature equilibrium is reached during logging operations.⁵⁰⁻⁵³

4. Results and Discussion

4.1 Source rock characteristics

4.1.1 Organic matter richness

The total organic carbon (TOC) content and the pyrolysis S_2 yields are the primary parameters that determine the effectiveness of the source rock in hydrocarbon generation and expulsion. The results indicate that the Manganhewa samples have a high TOC content of 0.68-90.02 wt. % (see **Table 1**), with most samples falling in the excellent source rock potential zone, as expected

since the sequence is rich in coal layers. The values of S_2 are 0.37-280.16 mg HC/g rock, and the (S_1+S_2) values range between 1.68 and 303.30 mg HC/g rock (see **Table 1**); these data indicate that the majority of the samples fall in the good to excellent zone, with excellent potential yield. These classifications are based on the system in Peters and Cassa.³ The hydrocarbon potentiality of the Manganhewa Formation has been evaluated using a TOC vs. S_2 cross-plot (see **Figure 3**). The diagram confirms that most of the assessed samples have excellent hydrocarbon quantity and production potential, with a clear distinction among the various lithologies.

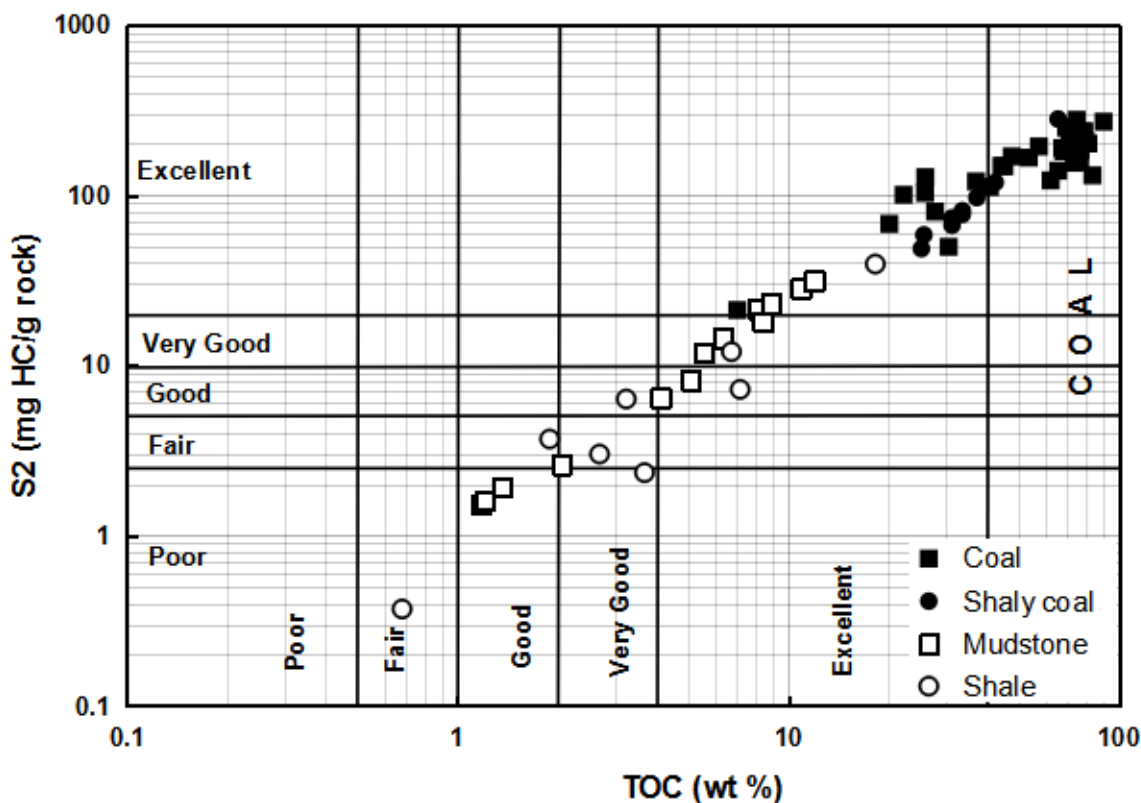


Figure 3. Cross-plot of total organic carbon (TOC) content versus pyrolysis S_2 yields, used to determine the source rock generation potential of selected samples from the Manganhewa Formation.

4.1.2 Types of organic matter

The hydrogen index (HI) is an essential parameter in the determination of the types of organic matter present in the source rock.² This can be attributed to the expulsion of hydrocarbons and subsequent decline in hydrogen content as the organic matter matures.

The HI values for the Manganhewa samples under study are between 54 and 491 mg/g TOC. According to the classification proposed by Peters and Cassa,³ most source rock samples are mixed Type II-III kerogen (oil and gas-prone) (44 samples), followed by Type II kerogen (oil-prone) (25 samples) and Type III kerogen (gas-

prone) (17 samples). The results obtained from this research study indicate that the presence of vitrinite-dominated coal with higher HI values is common not only in the Mangaheva Formation source rock samples, but also throughout the Taranaki Basin in New Zealand. This vitrinite is of a perhydrous nature, which can present a higher HI than expected and so be considered as a major source for the generation of liquid hydrocarbons. It has previously been concluded that not only liptinites, but also perhydrous vitrinites have the potential to generate hydrocarbon liquids in the course of natural coalification.⁹ It is also known that oil-prone

coals are mostly of Jurassic–Tertiary age in Australia, New Zealand, and Indonesia,⁹ which is in good agreement with the findings of this research.

The cross-plot of HI (S_2/TOC) versus OI (S_3/TOC) developed by Espitalié *et al.*⁵⁴ (see **Figure 4**), which is modified from the van Krevlen diagram in Tissot and Welte², was applied to identify the types of organic matter. The kerogen Type II-III mixed oil-/gas-prone is the most abundant type in the Mangaheva source rock samples.

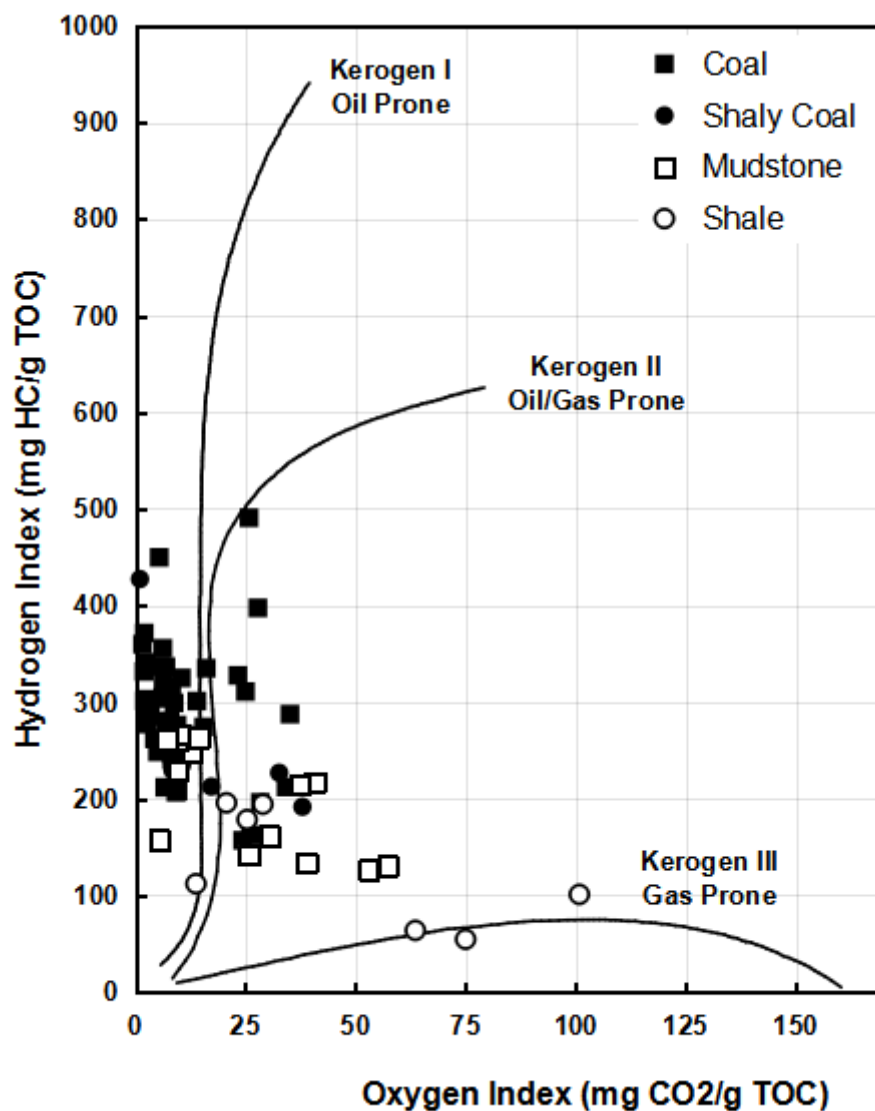


Figure 4. Van Krevlen diagram of oxygen index (OI) versus hydrogen index (HI), showing the generative type of selected samples from the Mangaheva Formation.

4.1.3 Palaeodepositional environment

4.1.3.1 Maceral composition

The petrographic description and quantitative maceral analysis for coal and shaly coal samples have been performed using MBIE and are summarized in **Table 3**. The quantification analysis of the coal and shaly coal Mangahewa source rock samples is predominantly composed of macerals of the vitrinite group, contributing

65% to 92.3% of the organic matter, with an average value of 85% (see **Table 3**). The ternary diagram (see **Figure 5**) for the maceral composition of selected coal and shaly coal samples indicates the prevalence of the vitrinite maceral group. Alginite and other liptinite maceral groups are observed in lower amounts (<20%) in the coal and shaly coal samples.

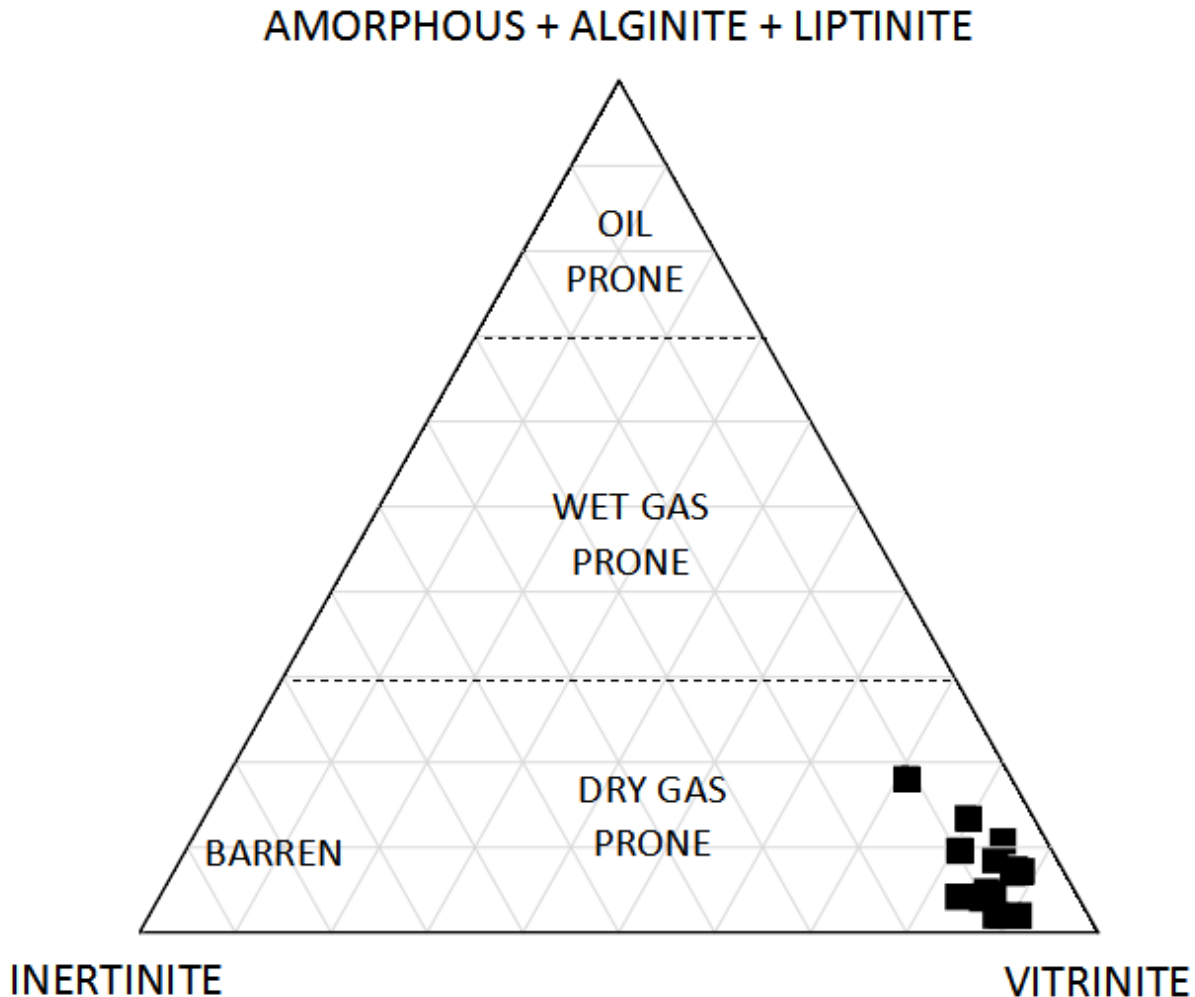


Figure 5. Ternary diagram showing the maceral composition of selected samples from the Mangahewa source rock.

Organic petrographic examination of selected shale samples reveals an abundance of alginite (see **Figures 6b, d and e**), followed by bituminite and solid hydrocarbon. The alginite assemblage recognized is telalginite, which retains the shape and morphology of the original algae.⁵⁵ These are macerals belonging to the liptinite group, which is believed to be produced from decayed leaf

matter, spores, pollen, and algal material, as well as from resins and plant waxes. Vitrinite macerals are rare (see **Figure 6a**); however, they seem to be indigenous, with smooth and clean surfaces ideal for reflectance measurements, whereas inertinite was not encountered. However, the predominant optically recognizable organic particles are solid hydrocarbons in the

form of migrabitumens mixed with clays (see **Figures 6c** and **f**), indicating the expulsion of oil. Pyrite occurs in both a massive form and frequently as framboidal (see **Figure 6e**). Traces of oil drops were also observed (see **Figures 6c** and **d**).

In general, the maceral distribution (see **Figure 5**) shows that vitrinite, most probably perhydrous in nature, is the predominant maceral group in

the coals and shaly coals, whereas alginite and bituminite are predominant in the more shaly strata. These findings suggest that the palaeodepositional environment of the Mangahewa Formation was a terrestrial one, with a minor marine influence. This is in good agreement with the geochemical and biomarker data, which shows kerogen Type II-III as the most abundant kerogen type. This can generate oil and/or gas at peak maturity.²

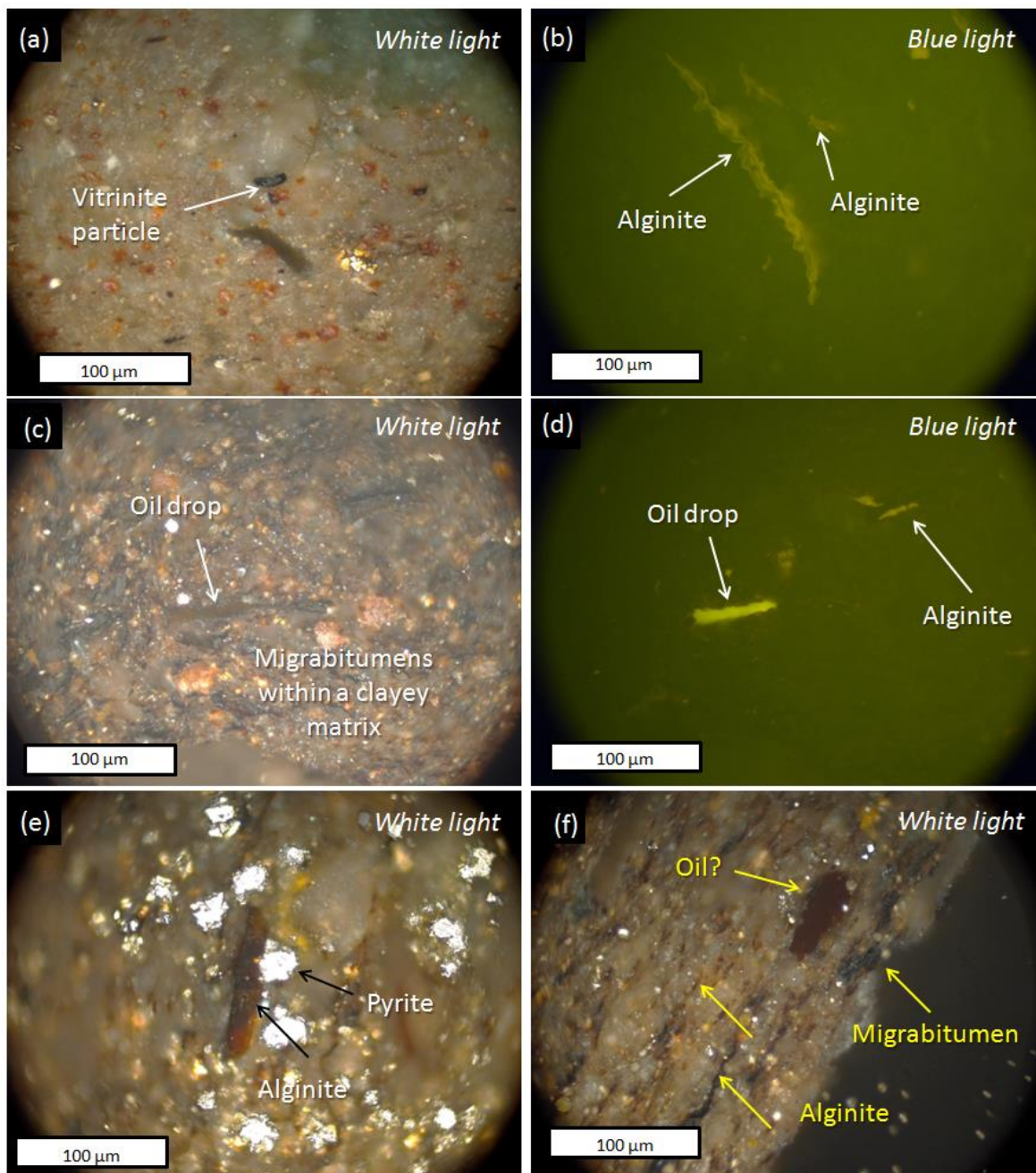


Figure 6. Photomicrographs of selected shale samples from the Mangahewa Formation, showing the presence of (a) vitrinite maceral (rare), (b,d,e,f) alginite maceral (common), (c,f) migrabitumen (abundant), (c,f) oil drop, and (e) pyrite.

The biomarker analyses and the distribution of n-alkanes indicate a mixed algal and terrigenous organic matter contribution, which is in good agreement with the RE and organic petrological results.^{56,57} The isoprenoid alkanes pristane (Pr) and phytane (Ph) are common biomarkers for fossil fuels.⁵⁸ They typically originate from phytyl side-chains in chlorophyll either under reducing conditions (phytane) or oxidizing conditions (pristane), and they function as good biomarkers due to their high resistance to degradation. It has already been established that

the Pr/Ph ratio can provide information about the degradation level of the petroleum residues, as well as the depositional environment. Values of Pr/Ph above 3 point to terrestrial sources.⁵⁸ The Pr/Ph values of the samples studied here are 2.68 to 13.35 (see **Table 4**), suggesting that terrestrial sources are dominant. The relationship between high Pr/C₁₇ (0.46-14.11) and low Ph/C₁₈ (0.14-3.4) values (see **Table 4**) is plotted in **Figure 7**, which shows an apparent predominance of land input to the organic matter.

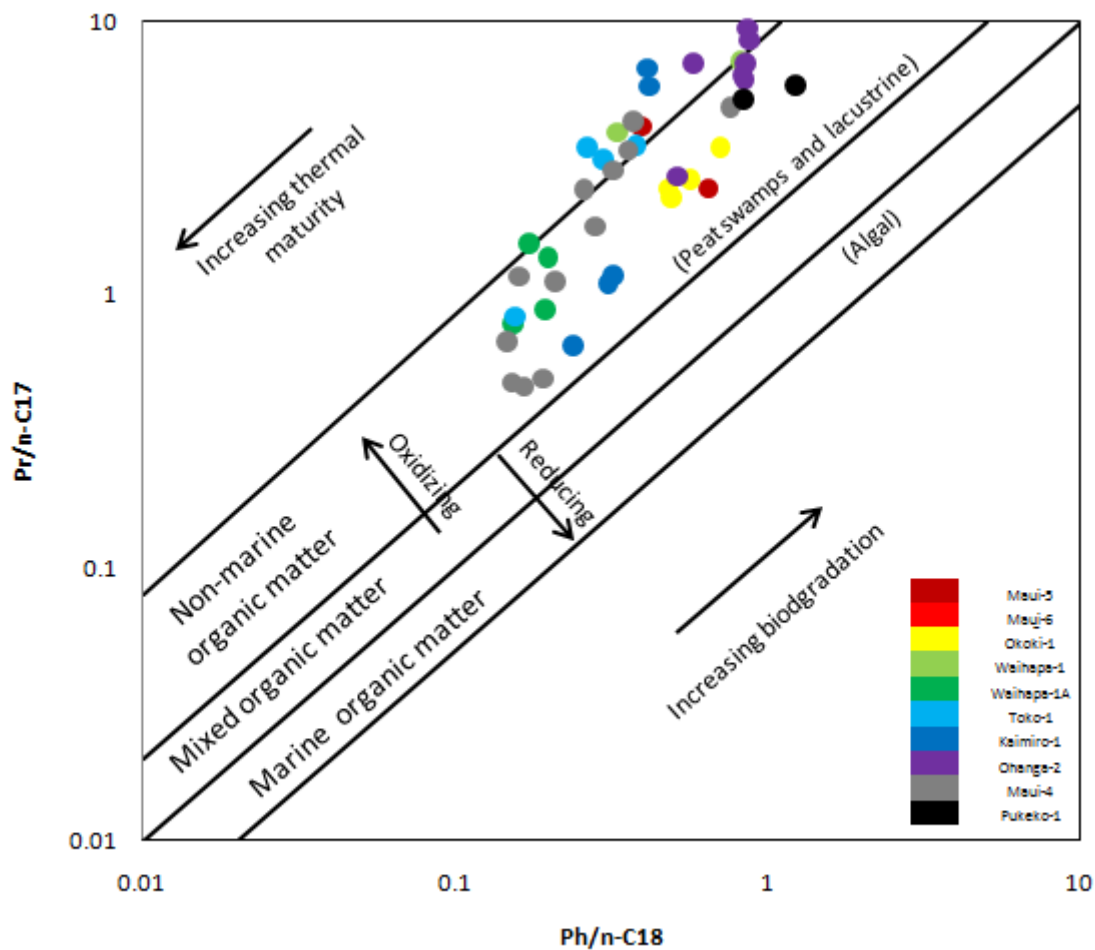


Figure 7. Phytane to n-C₁₈ alkane (Ph/n-C₁₈) versus Pristane to n-C₁₇ alkane (Pr/n-C₁₇) of selected samples from the Mangahewa Formation.

The degree of waxiness can be expressed by the ratio (sum of n-C₂₁ to n-C₃₁)/(sum of n-C₁₅ to n-C₂₀). Oils characterized by a high abundance of n-C₁₅ to n-C₂₀ n-alkanes in the saturate fractions have low waxiness and are typical of marine

organic sources, mainly higher plants deposited under reducing condition.⁵⁹ The samples studied here have waxiness values ranging from 0.46 to 9.06, with most samples above 1.0 (see **Table 4**); this high waxiness is characteristic of a terrestrial

origin. A cross-plot of Pr/Ph versus waxiness is shown in **Figure 8**, which reaffirms that the Mangahewa samples have a terrigenous origin with an oxidizing deposition environment, with few shifted samples as evidence of a marine reducing effect.

The terrigenous to aquatic ratio (TAR) is defined as the ratio of the contributions of terrigenous and aquatic plants. It is based on the relative abundances of long-chain (vascular plant) and

short-chain (algal) n-alkanes. In view of this, the ratio of the concentrations of (n-C₂₇+ n-C₂₉+ n-C₃₁) to (n-C₁₅+ n-C₁₇+ n-C₁₉) was examined and evaluated. **Table 4** shows that the TAR values of the samples are 0.09 to 11.55. There is a predominance of the long-chain n-alkanes C₂₇, C₂₉, and C₃₁, which is characteristic of a higher contribution from the plants in a terrestrial environment.⁶⁰ However, the TAR values may be misleading, as algal materials are susceptible to degradation.⁶¹

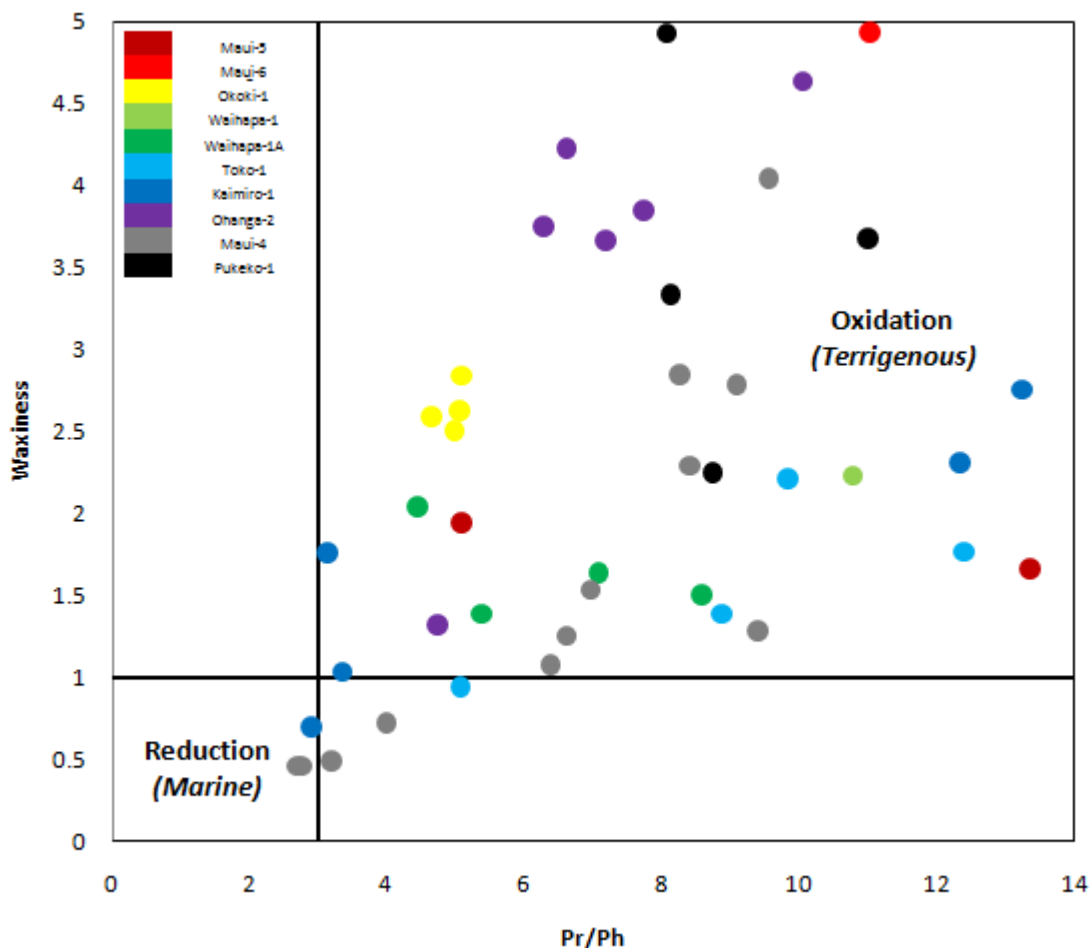


Figure 8. Pr/Ph versus waxiness cross-plot, used to determine the origin of the organic matter in selected samples from the Mangahewa Formation.

Results for tricyclic terpanes showed that the concentrations of C₂₃ tricyclic terpanes are generally low, as demonstrated by the high values for the ratio C₁₉/C₂₃ (0.1-98.31) and the low values for the ratio C₂₄/C₂₃ (0.0-1.30). This may also indicate that the samples are mainly of terrestrial origin⁶² (see **Table 5**).

Peters, Walters and Moldowan⁵⁶ have concluded that gammacerane abundance is a good indicator of source sediments deposited in hypersaline lakes. The presence of gammacerane is a unique characteristic of hypersalinity-induced water-column stratification during deposition. An

oxidizing, non-marine origin can therefore be inferred from the very low levels of gammacerane (0.0-0.06) (see **Table 5**).

A predominance of C₂₇ steranes over C₂₈ and C₂₉ steranes typically indicates marine-sourced organic matter, which is not observed in the samples from the Mangahewa Formation analyzed here. The samples show that C₂₉ steranes are dominant, which suggests the input of advanced plants⁵⁶ (see **Table 6** and **Figure 9**).

As most of the samples examined were coals, which represent the deposits of terrestrial plants, the laboratory results are in accordance with the lithological nature of the samples. The overall

results from both the organic petrography and the biomarker assessments indicate that the Mangahewa Formation samples contain organic matter of terrigenous origin deposited in a terrestrial environment, with only limited marine influence. This is characteristic of “paralic coals”, which originate in a body of water once linked with the open sea. Furthermore, combining the detected biomarkers with the relatively high HI, obtained from the Rock-Eval data, and the predominance of vitrinite, as shown from the petrographic data, it can be inferred that the coals under examination have a perhydrous character, which has contributed to the release of liquid hydrocarbons.

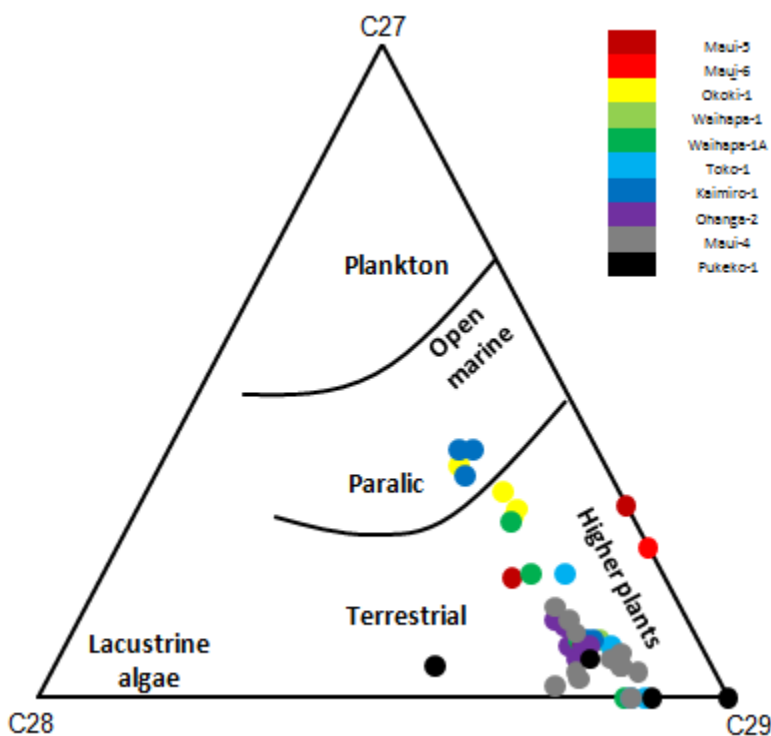


Figure 9. The depositional environment of the Mangahewa samples, as inferred from the ternary diagram for C₂₇, C₂₈ and C₂₉ steranes, showing the dominance of C₂₉ steranes.⁷⁴

4.1.4 Thermal maturation and hydrocarbon generation

The data for the maximum temperature T_{max} and vitrinite reflectance (VR%) have been assessed to determine thermal maturity. The values of T_{max} vary according to the maturity of the different types of organic matter.³⁸ Following earlier studies by Sykes and Snowden⁸ and Barker,⁶³ a minimum T_{max} value of 430°C has been

considered necessary for the thermal maturation of source rocks. The Mangahewa samples have T_{max} values in the range 414–447°C, indicating an immature to early mature stage.³

Figure 10 shows the cross-plot of HI versus T_{max}, which allows the thermal maturity of the Mangahewa Formation to be evaluated. For the

majority of source rock samples the value of T_{max} lies above 430°C , indicating the oil window and a source rock that is thermally mature. The VR% of 35 well samples ranges from 0.51 to 0.87%, with most samples above 0.55% (see *Table 2*).

This also suggests that the selected samples are thermally mature. The distribution of T_{max} versus VR% is plotted in *Figure 11*, which indicates that the samples are immature to mature, in good agreement with *Figure 10*.

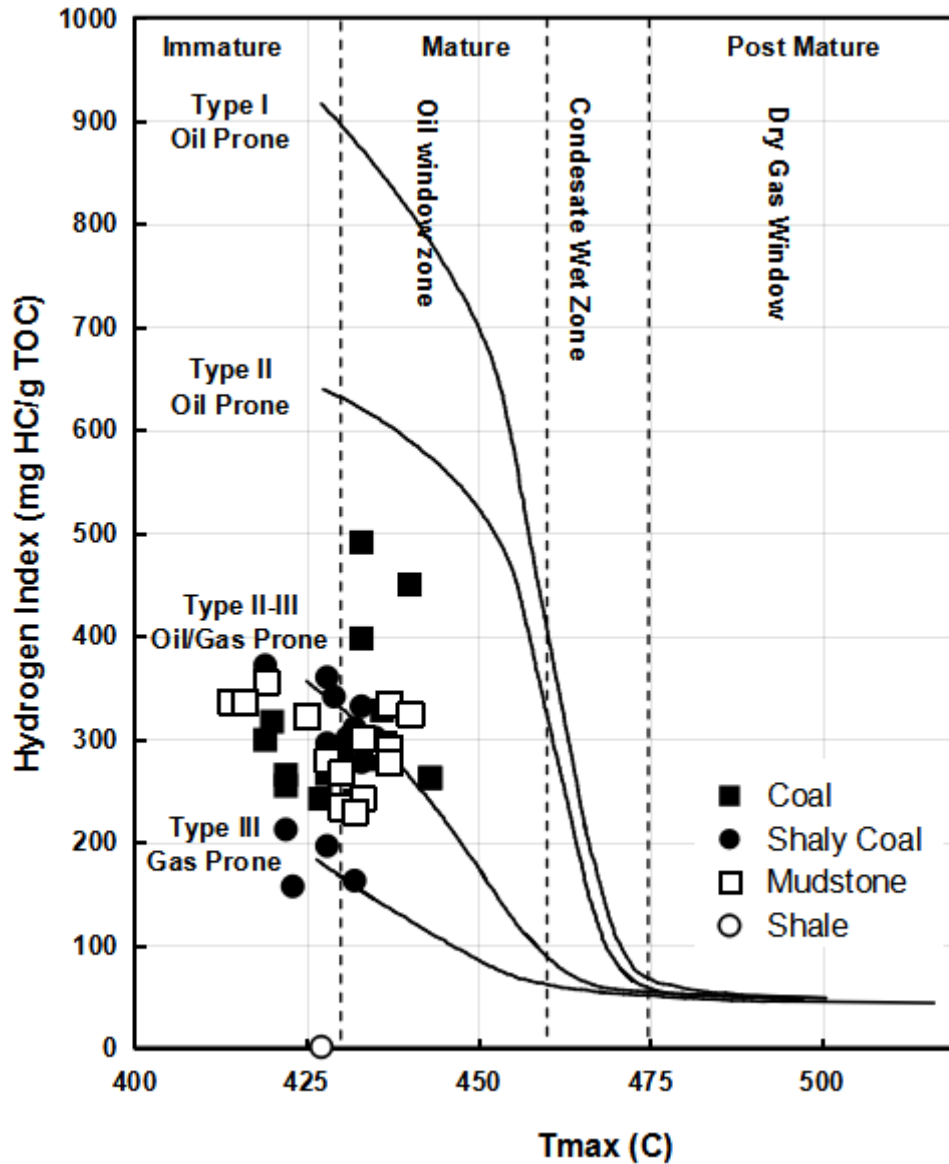


Figure 10. Plot of Pyrolysis T_{max} as a maturity parameter versus HI, indicating the relationship of the maturity level to the kerogen type in selected samples from the Mangahewa Formation.

The types of hydrocarbon generated can be inferred from a cross-plot of the production index (PI) and T_{max} (see *Figure 12*). Many of the data points indicate that the hydrocarbon generation is of indigenous origin, while others appear along the margins of the indigenous hydrocarbon generation zone. This suggests pre- to early

maturity. Data points with T_{max} below 430°C indicate an immature stage, and are plotted outside the indigenous hydrocarbon generation zone. The identification of solid migrabitumens within the matrix of the shale samples, but not in the cracks (see *Figure 6*), provides further proof of indigenous hydrocarbon generation.

In addition, the biomarker parameter C_{32} homohopane can be used as a maturity indicator. The sample value is 0.33 (see **Table 5**), which suggests immaturity of the organic matter contained in the sample studied. This is supported by the C_{29} sterane biomarkers, which are also used as maturity indices in this study. The ratio of C_{29} 20S/(20S + 20R) steranes increases from 0 to 0.5 with increasing thermal

maturity, which in turn causes an increase in the ratio C_{29} $\beta\beta/(\alpha\alpha + \beta\beta)$ steranes to ~ 0.7 .^{64,65} At higher levels of maturity, this ratio remains constant as it is independent of the input of organic source matter.⁵⁶ **Figure 13** shows the relationship between the two parameters, which confirms that the samples belong to the immature to mature stage.

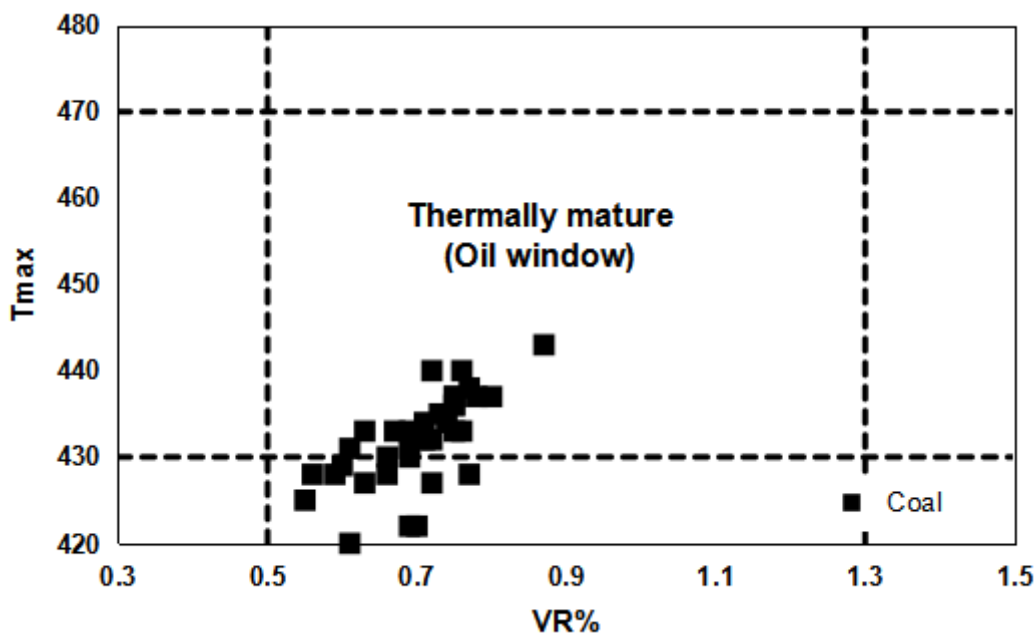


Figure 11. Plot of the organic maturity parameters vitrinite reflectance versus T_{max} , confirming the maturity levels of selected samples from the Mangahewa Formation.

4.2 Reservoir characteristics

4.2.1 Petrophysical analysis and reservoir quality

The porosity and permeability values of the selected core samples from the Maui-5, Maui-6, MB-P(8), and Moki-1 wells in the Mangahewa Formation are listed in **Table 7**. The results show a good positive relationship between the porosity and permeability values, suggesting that migration pathways increase with an increasing amount of pore space (see **Figure 14**). The overall porosity range is from 9.5% to 24.9% (with a mean of 18.2%). The permeability values range from 1.2 mD to 6900 mD (with a mean of 1678.9 mD). A histogram has been plotted showing the permeability and porosity values in the Mangahewa reservoir samples (see **Figure**

15). Most samples have more than 15% porosity and 100 mD permeability. According to Levorsen,⁴⁷ samples with these porosity and permeability values are classified as very good. Hence, the petrophysical data shows that the Mangahewa Formation has promising reservoir quality.

4.2.2 Sedimentological study and petrography of the reservoir rock

The thin sections selected from the Maui-5, Maui-6, and Maui-7 wells collectively show a number of characteristics when examined under the petrographic microscope. Various features have been observed, from good pore spaces to defective diagenetic features.

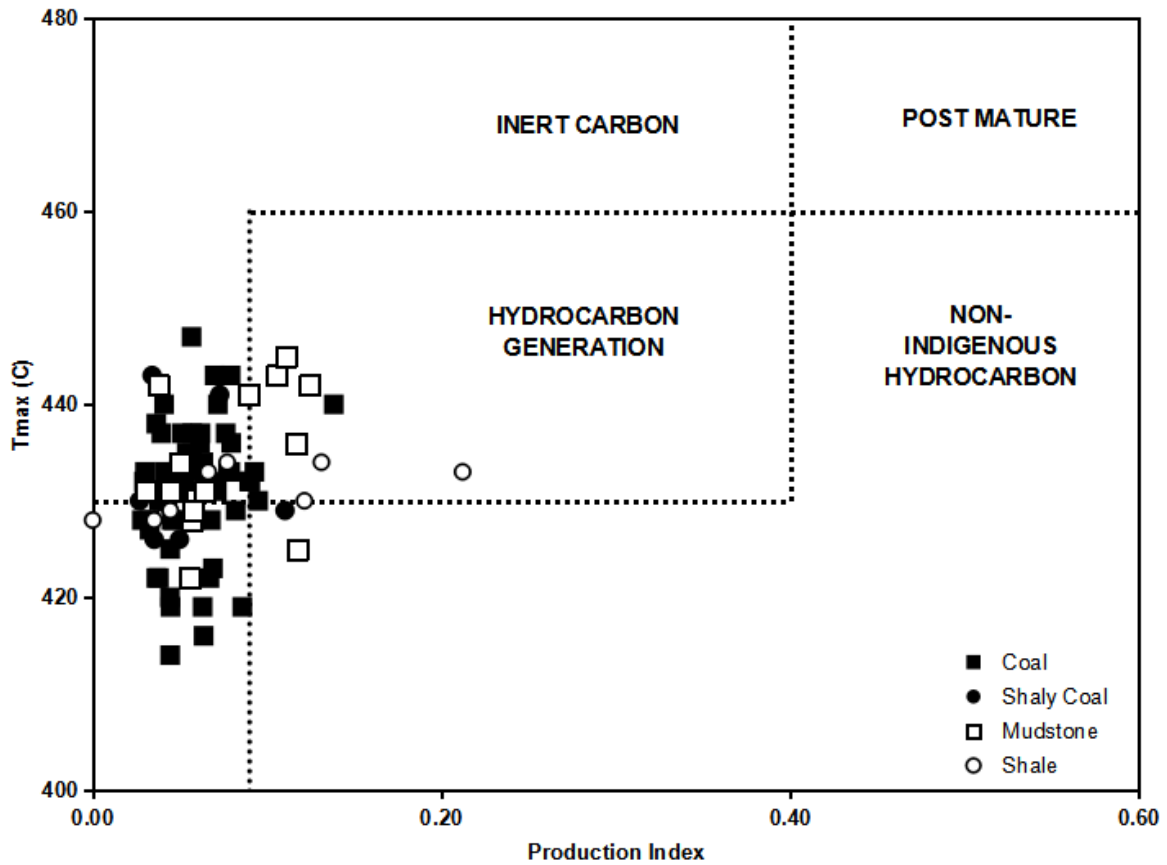


Figure 12. Cross-plot of T_{max} versus production index (PI), showing the nature of the hydrocarbons in selected samples from the Mangahewa Formation.

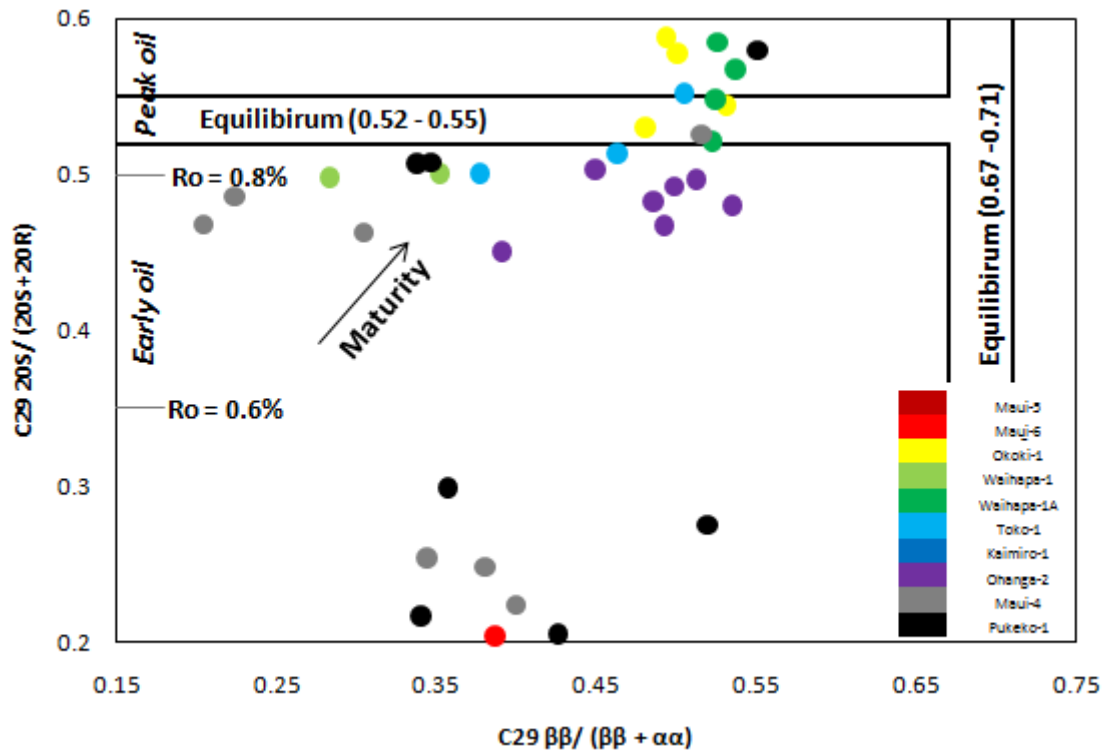


Figure 13. Maturity determination cross-plot using C_{29} steranes.

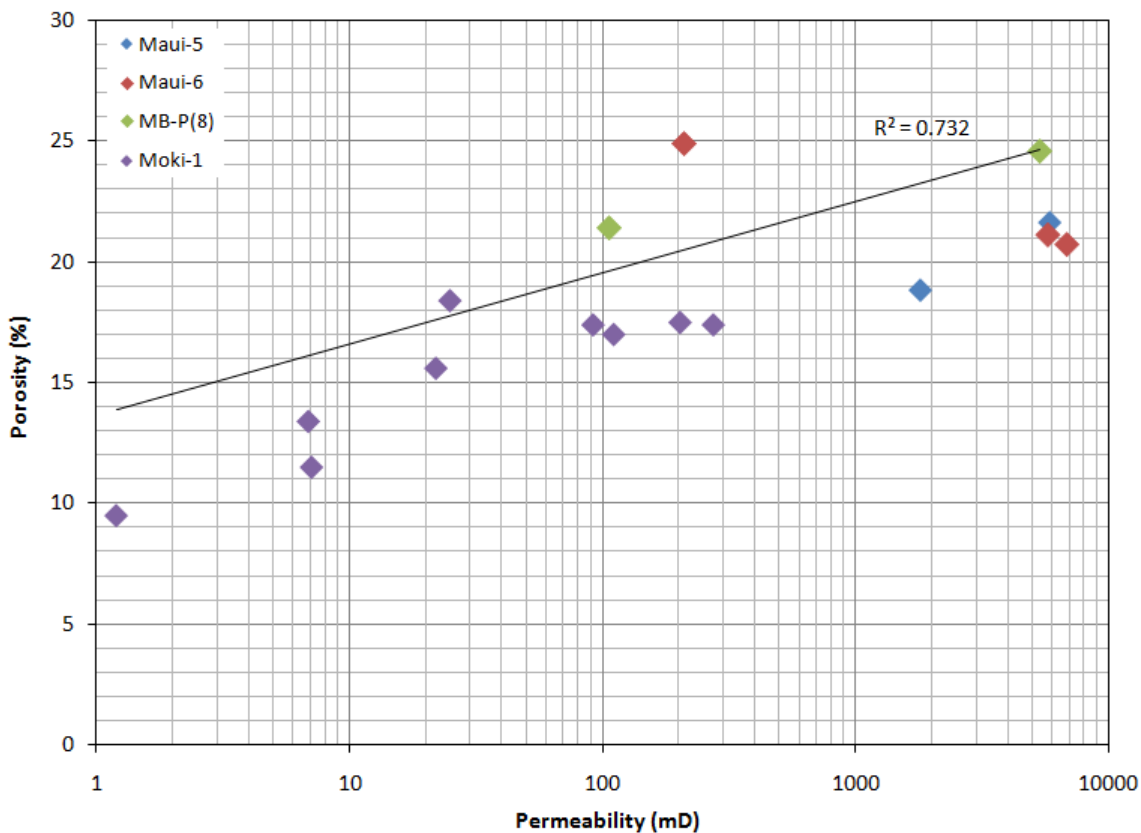


Figure 14. Relationship of the porosity to the permeability for selected Mangahewa reservoir samples, showing a positive trend.

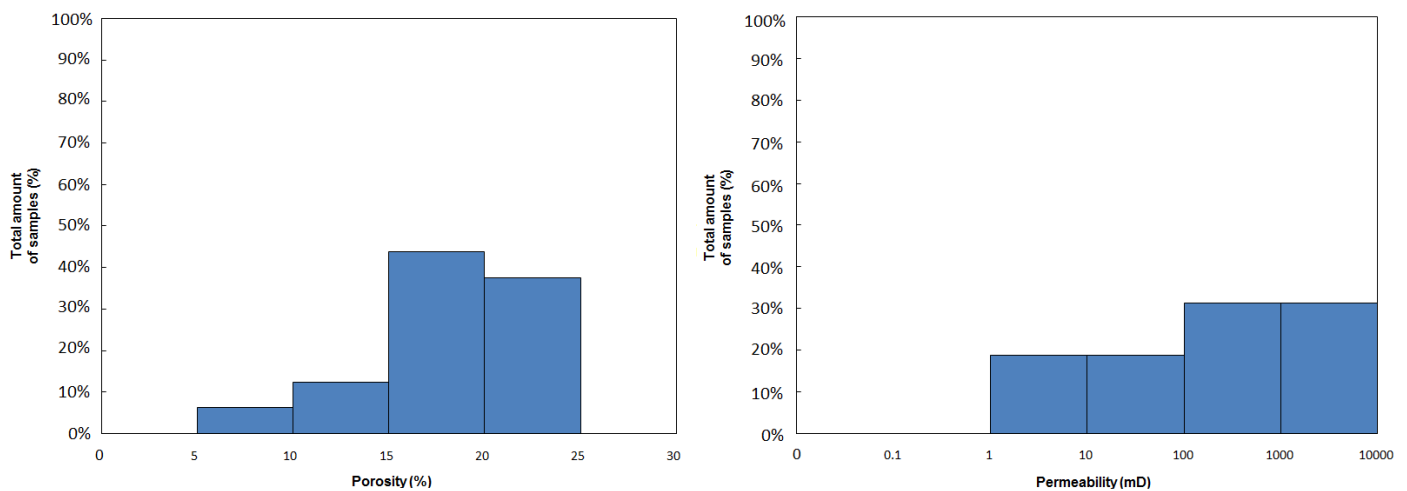


Figure 15. Porosity and permeability histograms for the Mangahewa reservoir rock in the wells under study.

A good reservoir should possess abundant porosity. This is the case for the Mangahewa samples studied here. The grains are loosely packed and at least moderately well sorted, while the pore spaces are found in large quantities (see *Figures 16A-F*). Both primary intergranular and secondary dissolution pores have been observed

in abundance in the selected samples. It is vital for these pore spaces to be well connected for a reservoir to be efficient. The absence of potential migration pathways, even in the presence of pores, would inhibit the production potential. Well-connected porosities enhance the effective porosity and permeability.^{27,66-68} Effective pores

result in good permeability. This is shown by the ubiquitous hybrid pores observed in the photomicrographs in **Figures 16A-F**. This hybrid porosity is formed when the dissolution merges with the intergranular pores forming an effective porosity. This effective porosity supports the previous results concluded from the

petrophysical analysis of the core dataset, where a positive relationship was observed between porosity and permeability (see **Figure 14**). In addition, good permeability values have been observed in selected core samples (see **Figure 15**).

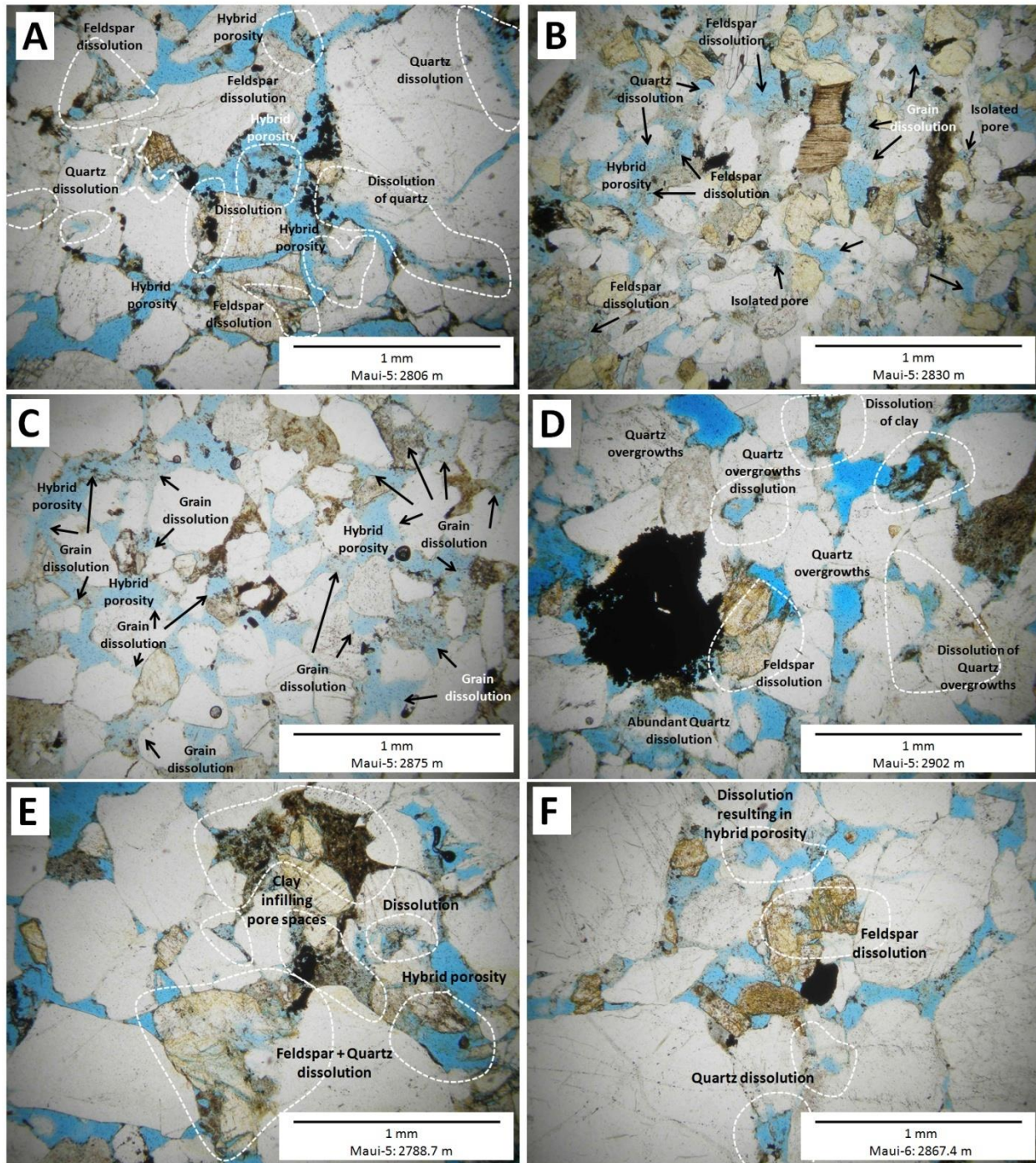


Figure 16. Photomicrographs showing features observed in selected Mangahewa Formation samples: (A)-(F) Abundant primary intergranular porosity (stained blue), secondary dissolution in feldspar and quartz, and hybrid porosity.

The process of compaction typically contributes to poor reservoir performance. This is because the associated features of compaction and diagenesis generally reduce porosity and permeability. In the selected thin sections, cementation has been observed at various points. The main cementing agents are calcite and clay. Calcite cementation can be observed occluding the pore spaces between grains in **Figures 17 B-E**.⁶⁸⁻⁷⁰ In the thin sections studied here, clay minerals occlude the pore spaces, act as pore

lining and replace minerals. In **Figures 17C-E**, clay minerals are observed to fill in what likely were originally pore spaces between mineral grains and act as a strong cementing agent. Clay minerals have also been observed to replace minerals, as in **Figures 17D-E**. In addition, clay minerals such as chlorite and muscovite can be seen in **Figures 17C-D**. Due to the ductile nature of these clay minerals, they are successful pore-blocking features where they are present in large quantities.

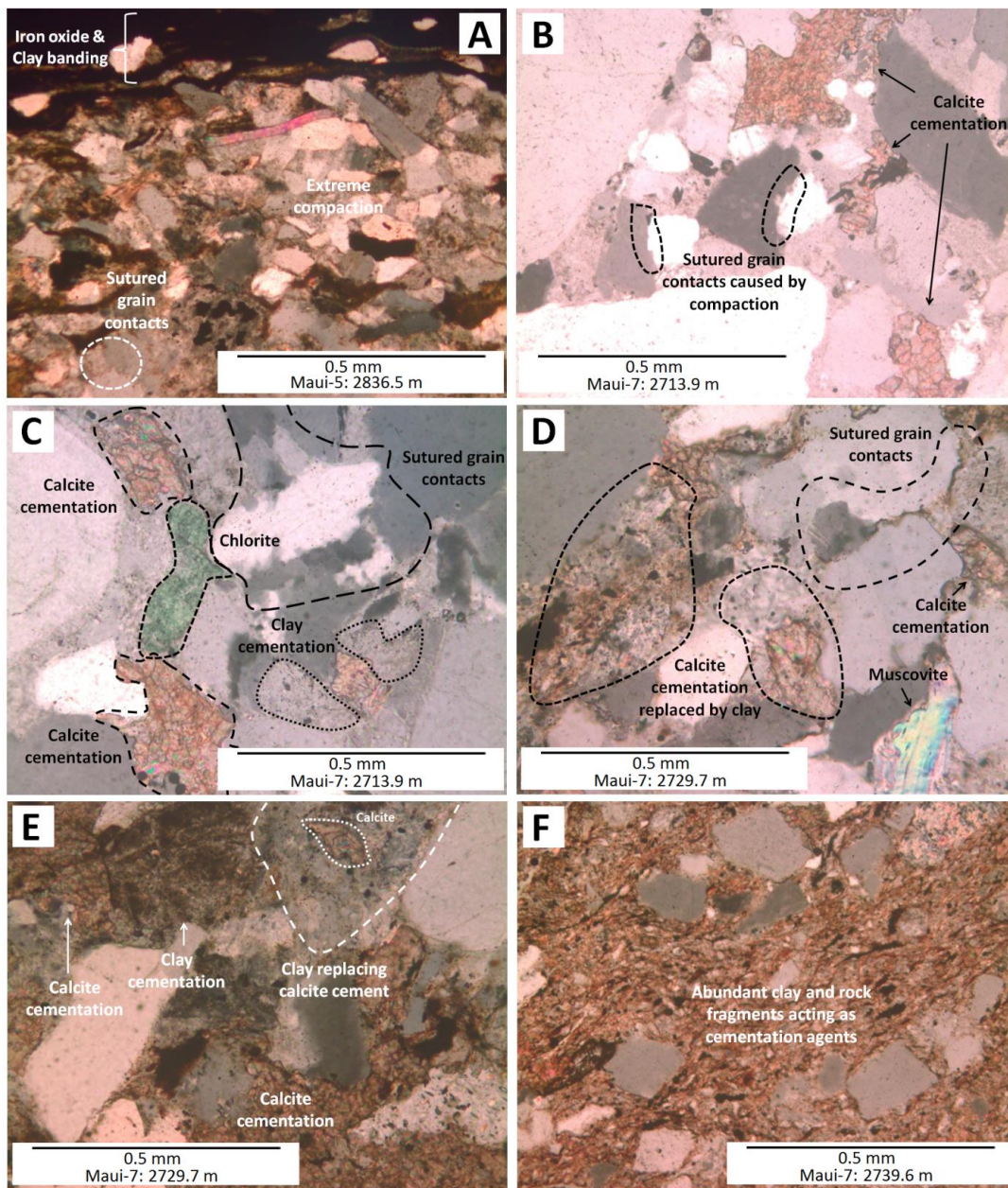


Figure 17. Photomicrographs showing features observed in selected Mangahewa Formation samples: (A-F) Extreme compaction depleting pore spaces and abundant cementation by clay, calcite and rock fragments.

Examination of the petrographic thin sections also indicates that the samples have been subjected to severe mechanical compaction. This is particularly evident where diagenetic features have been observed, such as long and point grain contacts and sutured contacts between grains, as well as dissolution and fractures of the quartz grains. These features have all been observed in some parts of the thin sections under study.⁶⁸⁻⁷⁰

Figures 17A-D show the great extent of compaction, where the aforementioned diagenetic features have been identified. Banding of iron oxide and clay has also been observed in **Figure 17A**, as a result of compaction.

Although various diagenetic features have been observed, they have been eclipsed by the abundance of effective pores in most parts of the thin sections studied. The results of the thin

section examinations agree with the petrophysical data analysis discussed above, which suggested good reservoir qualities, with good porosity and permeability values.

The selected core samples from the Maui-5, Maui-6, and Maui-7 wells have been found to further support the conclusions drawn previously from the thin section examination. The scanning electron microscope analysis shows consistency, with abundant porosity observed from the thin sections (see **Figure 18D**). The clay mineral kaolinite was also observed to be present between mineral grains and exhibits a booklet-like texture (see **Figures 18A-C**). The kaolinite particles infill pore spaces and hence negatively affect the effective porosity and permeability, and the reservoir performance as a whole.

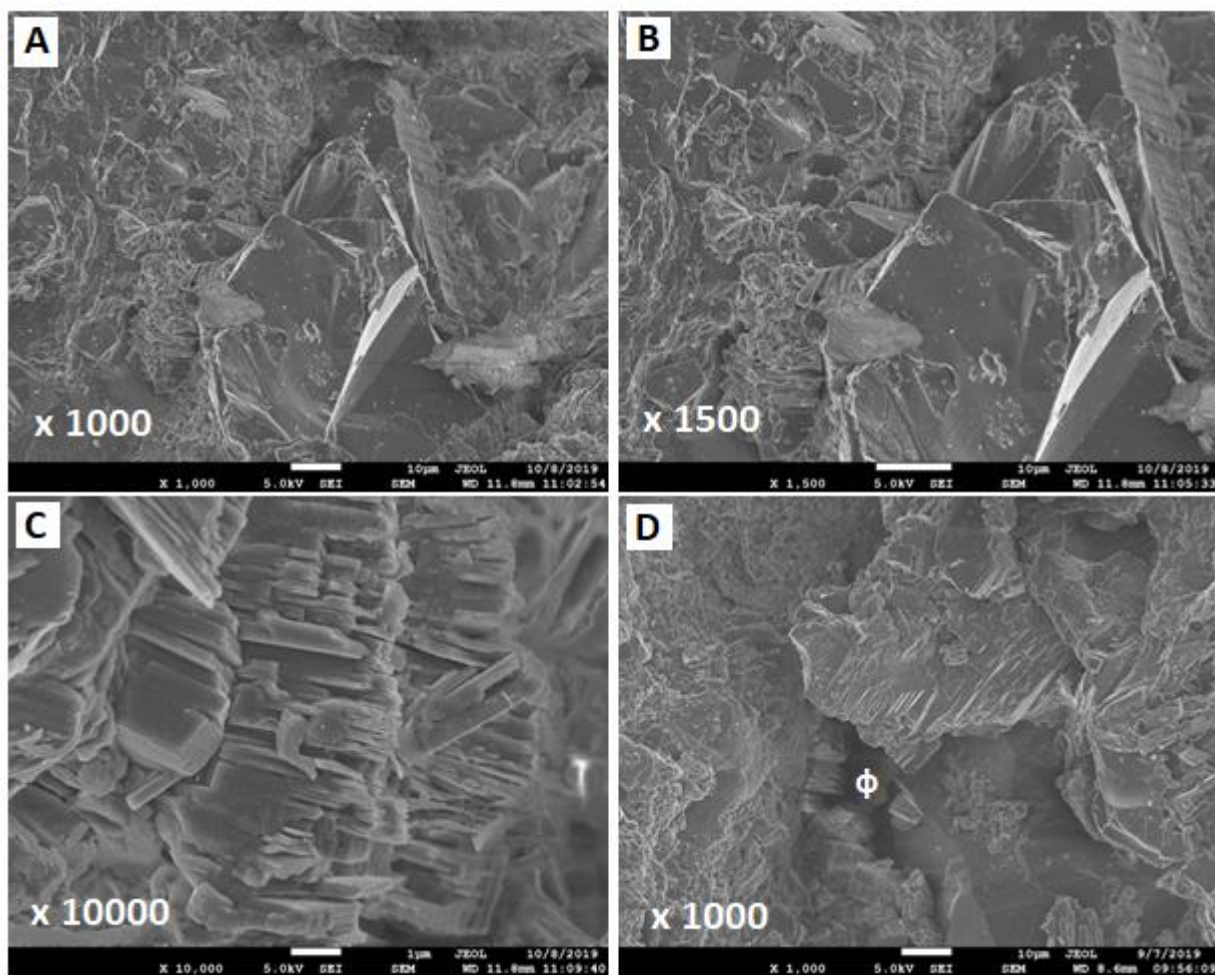


Figure 18. SEM images at different magnifications showing features observed in selected Mangahewa Formation samples: (A-D) Kaolinite clay particles forming booklet-like texture between Quartz grains, (D) Pore spaces between grains.

4.2.3. Well log interpretation

The principal aim of well log analysis is to examine the hydrocarbon potentiality of the reservoir units. Each well was first examined to identify potential reservoir zones within the section of the Mangahewa Formation penetrated by the wells. In a clastic reservoir, the expected reservoir lithology is sandstone, which has low radioactivity due to low clay mineral content. Hence, reservoir zones can be identified based on these characteristics, via a combined interpretation of the Gamma-ray and Neutron-Density logging curves. Low Gamma-ray values are indicative of low organic matter content, and negative separation between the neutron and density log curves is characteristic of a sandstone lithology.^{71.72}

Lithology identification is aided by the use of Neutron-Density cross-plots (see **Figure 19**). The cross-plots confirm that the reservoir zones for all wells have mostly sandstone lithology, but the Maui-7 well in particular shows a hint of other lithologies besides sandstone. In this well, the lithology of the Mangahewa formation may be attributed to the presence of calcareous sandstones, due to the ubiquity of calcite cementation. In addition, the variant lithology may also be a result of a large amount of fine-grained sediments and clay cementation. Their presence can be seen in the photomicrographs in **Figure 17**.

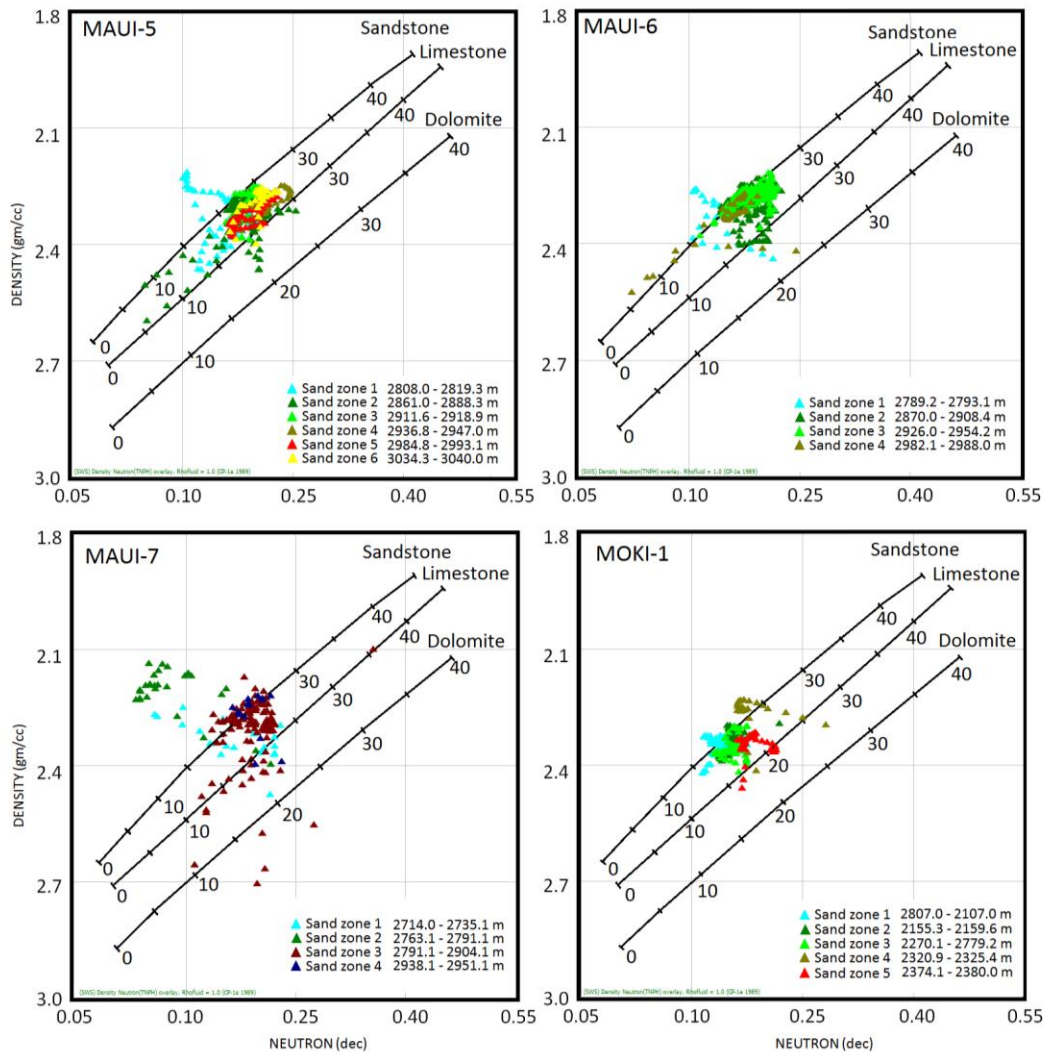


Figure 19. Neutron-Density crossplot showing the lithology and porosity analyses of four wells in the reservoir zones in the Mangahewa Formation.

Once the reservoir zones have been identified, the clay volume and type within the zones are evaluated. The clay volume is calculated using single-clay indicators of gamma-ray and resistivity logs and double-clay indicators of neutron-density logs. The clay volume used is the lowest volume produced by the indicators.⁷³ For the four wells selected, the clay volume quantified by the gamma-ray logs has the lowest and most stable values. Clay type determination is important because different clay structures within a unit (dispersed, laminated, and

structural) have varying effects on the formation fluid pressure, and therefore affect the effective porosity and water content significantly.⁷³ Depending on the clay type present, the wells are then analyzed using either a dual water saturation model (dispersed clay) or simandoux saturation model (laminated clay). The clay type identified in this paper, as dictated by the neutron porosity against density porosity cross-plot in **Figure 20**, is dispersed clay for all four wells. Hence, they have been treated using the dual water porosity-saturation model.

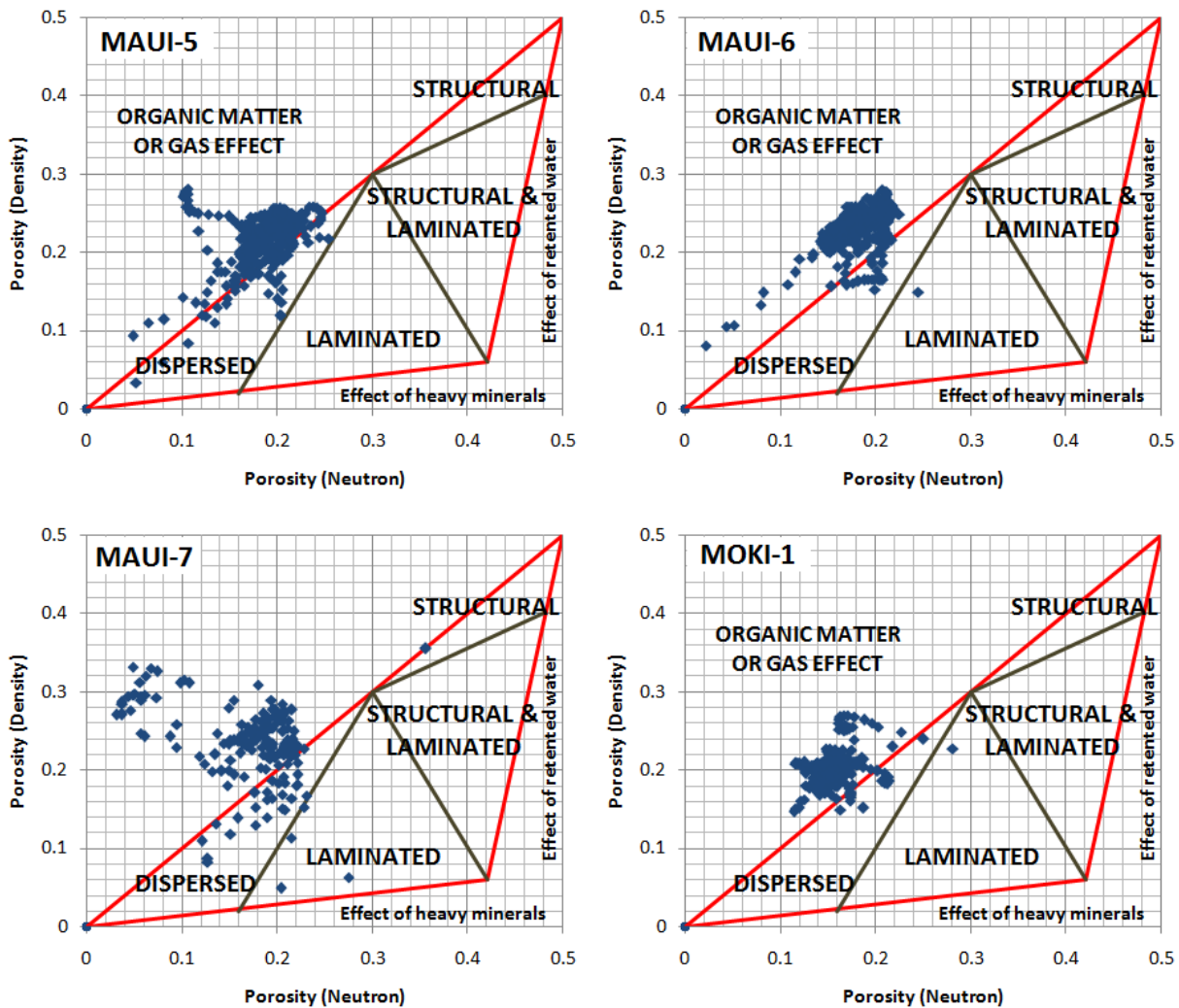


Figure 20. Diaporosity crossplots showing the clay type analyses for four wells in the Mangahewa Formation.

The Mangahewa Formation shows promising reservoir quality based on the overall results of the well log analyses made on the four drilled wells under study, following research previously done by Shalaby *et al.*²⁸ and Qadri, Islam and

Shalaby^{73,74}. The computed average petrophysical values from the four wells examined are listed in **Table 8**. The total average porosity ranges from 17.9% to 21.8% (with a mean of 21.3%), with effective pores making up

13.0% to 17.57% (with a mean of 15.7%). The types of pores present in the reservoir rock samples are identified from the cross-plot between the sonic and neutron-density porosities (see **Figure 21**). It can be seen that the pores are mostly of primary intergranular type. The volumes of clay present in these pay zones range

between 17.6% and 32.7%, averaging at 28.2%. The Mangahewa Formation shows low water saturation, with the lowest value 18.4% and highest 44.7%, and an average value of 32.1%. Thus, the average hydrocarbon saturation is high with a mean value of 67.9% (see **Table 8**).

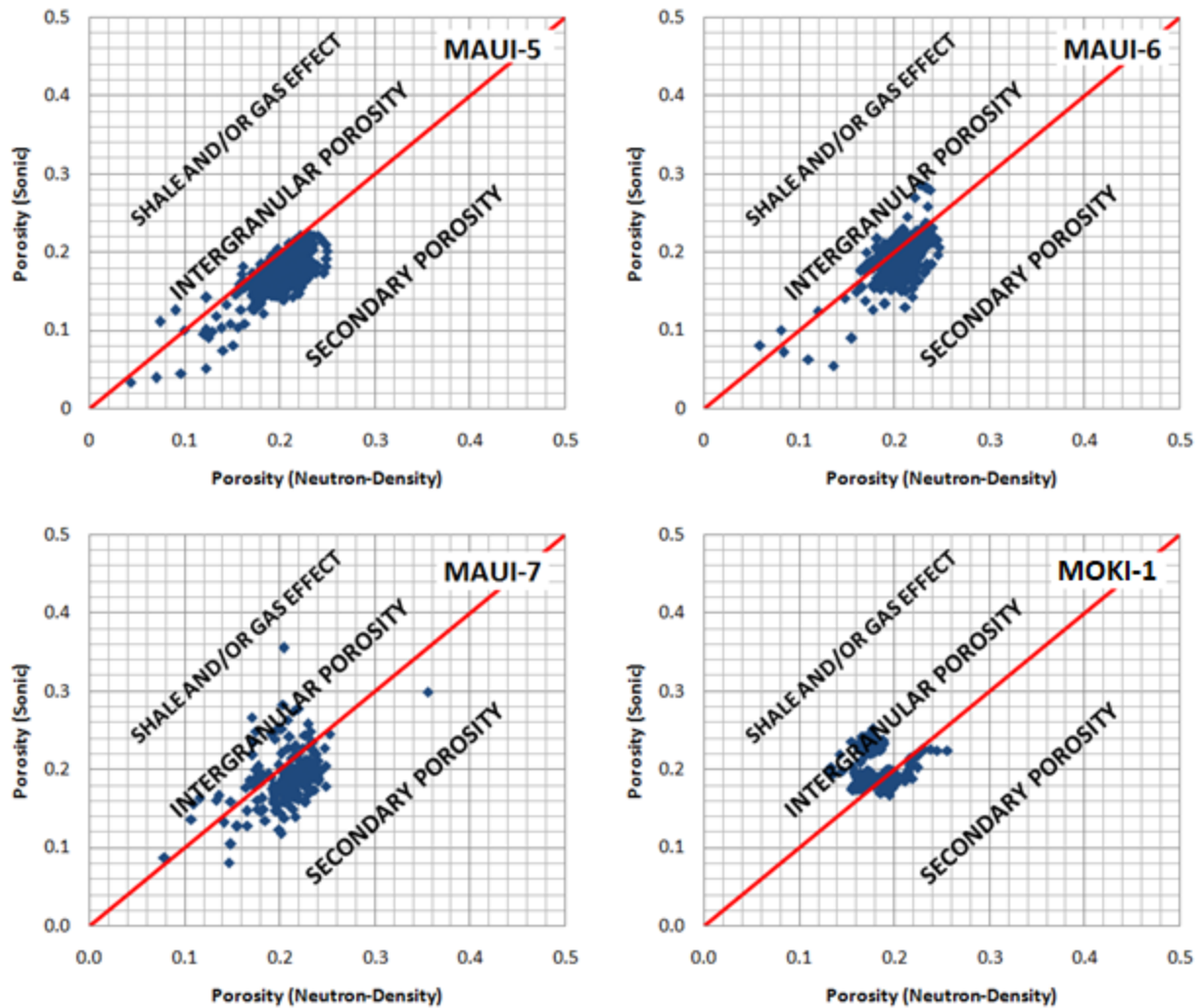


Figure 21. Total porosity types for the Mangahewa Formation sandstones.

The best producing well is the Maui-7 well, where three producing reservoir zones have been interpreted (see **Figure 22**). This well has a total of 19.5 m net pay thickness. The average clay volume is 32.6% and the average effective porosity is 16.3%. The average hydrocarbon saturation is 81.6%. Oil-water contact (OWC) is predicted to be found at 2807 m. This is supported by the change in resistivity separation above and below this contact. Big separations

indicate the presence of hydrocarbons, which are typically non-conductive fluids and hence show high resistivity values. The best pay zone is Zone 2, where the hydrocarbon saturation reaches 92.1%, with a good effective porosity (16%).

4.3. 1D basin modeling and timing of hydrocarbon generation

A one-dimensional basin modeling diagram has been constructed for the Cardiff-1 Well using the

Petromod software provided by Schlumberger. The model is used to examine the timing and depth of hydrocarbon generation and expulsion for the source rock of the Mangahewa Formation. The Cardiff-1 Well penetrates several formations from top to bottom. The burial history chart and sedimentation rate indicate that the Mangahewa Formation (the zone of interest) is encountered at a depth of 4062m, as the deepest formation at the bottom, with a great thickness reaching 1002m. The formation was deposited in time intervals of 6my, with a rate of sedimentation of around 167m/my. The lowest sedimentation rate has been recorded in the Turi Formation which is estimated at 1m/my, while the maximum rate of sedimentation is observed in the Matemateaonga Formation to be about 460m/my. The top of the oil window for the Mangahewa Formation in the Cardiff-1 Well is detected at 18.8 Ma ago at a depth of 2900m from the surface (see **Figure 23**). The organic source rock has attained enough maturity to generate gaseous hydrocarbon at a depth of 3220 m at 16.2Ma ago. It is observed that the postmature condensate zone is reached at a depth of 4920 m at 3.7 Ma ago (see **Figure 23**). **Figure 24** reflects the hydrocarbon transformation ratio for the Mangahewa Formation, which indicates that oil has been generated in concentrations ranging from 22mgHC/gTOC at 18Ma ago to 49mgHC/gTOC at 15Ma ago. The generated gas has a TR% of from 4mgHC/gTOC at 18Ma ago to around 10mgHC/gTOC at 15Ma ago. From the results of the expulsion ratio models, the ratio between the oil and gas generated by the source rock may be determined. This in turn indicates the kerogen type present, as well as the state of thermal maturity of the source rock. The expulsion ratio model for the Cardiff-1 well shows that the formation expelled both kerogen type II-III and type III, which suggests a mixture of both oil and gas in the hydrocarbon generation.

4.4. Petroleum system

The main outcomes of this research study have so far established a good understanding of the petroleum system of the Mangahewa Formation, in terms of the source potential and reservoir quality. The results have shown that the

Mangahewa source rocks possess excellent quantities of organic matter, and a portion of the source rocks have attained enough maturity for hydrocarbon expulsion. The reservoir rocks have good porosity and permeability to host hydrocarbons. In addition, the textural and diagenetic properties indicate a high reservoir quality. Nonetheless, without a good seal the hydrocarbons would continue migrating upwards from the reservoir rock to the surface.

In the Taranaki Basin, the mudstones are the primary seal rocks, and they are found to be widespread across the basin. The mudstones were deposited during periodic marine incursions and eventual transgression over the coastal plains during the Late Cretaceous and Paleocene. The main regional seal units are mudstones of the Turi and Manganui formations,⁷⁵ which are present as either (i) reservoir-seal pairs via intercalation with sandstones in the Palaeocene and Miocene, or (ii) stacked, thin intra-formational mudstone seals in otherwise thick sandstone reservoirs of Palaeocene and Eocene age.⁷⁵ Field *et al.*⁷⁵ performed a seal quality study in Taranaki Basin, which included the Maui-4 and Maui-3 wells, both in the area of the Maui Field. The results of seismic studies covering some parts of the study area indicate good seals in the upper part of the Cretaceous (the North Cape Formation) and in the Late Oligocene-Early Miocene interval. They also indicate that good seal characteristics have been observed in the Upper Eocene, Oligocene and parts of the Miocene units. These results support the likelihood that the Turi Formation seals the Mangahewa sandstone reservoir.

A hypothetical sketch diagram showing simplified subsurface structural configurations and the petroleum system elements, taking into account data from selected nearby wells, is shown in **Figure 25**.⁷⁶ The hydrocarbon migration generally follows the direction of least pressure, which is usually but not necessarily upward in the stratigraphic sequence. As a whole, the movement of hydrocarbons within the Taranaki Basin source-reservoir systems is poorly known. Migration pathways are likely

short and are generally assumed to involve bedding plane or fault plane conduits, or combinations of both.³⁰ Therefore, the migration pathways are expected to take place

stratigraphically across the bedding planes within the Mangahewa Formation and/or structurally through the faulted permeable zones (see *Figure 25*).

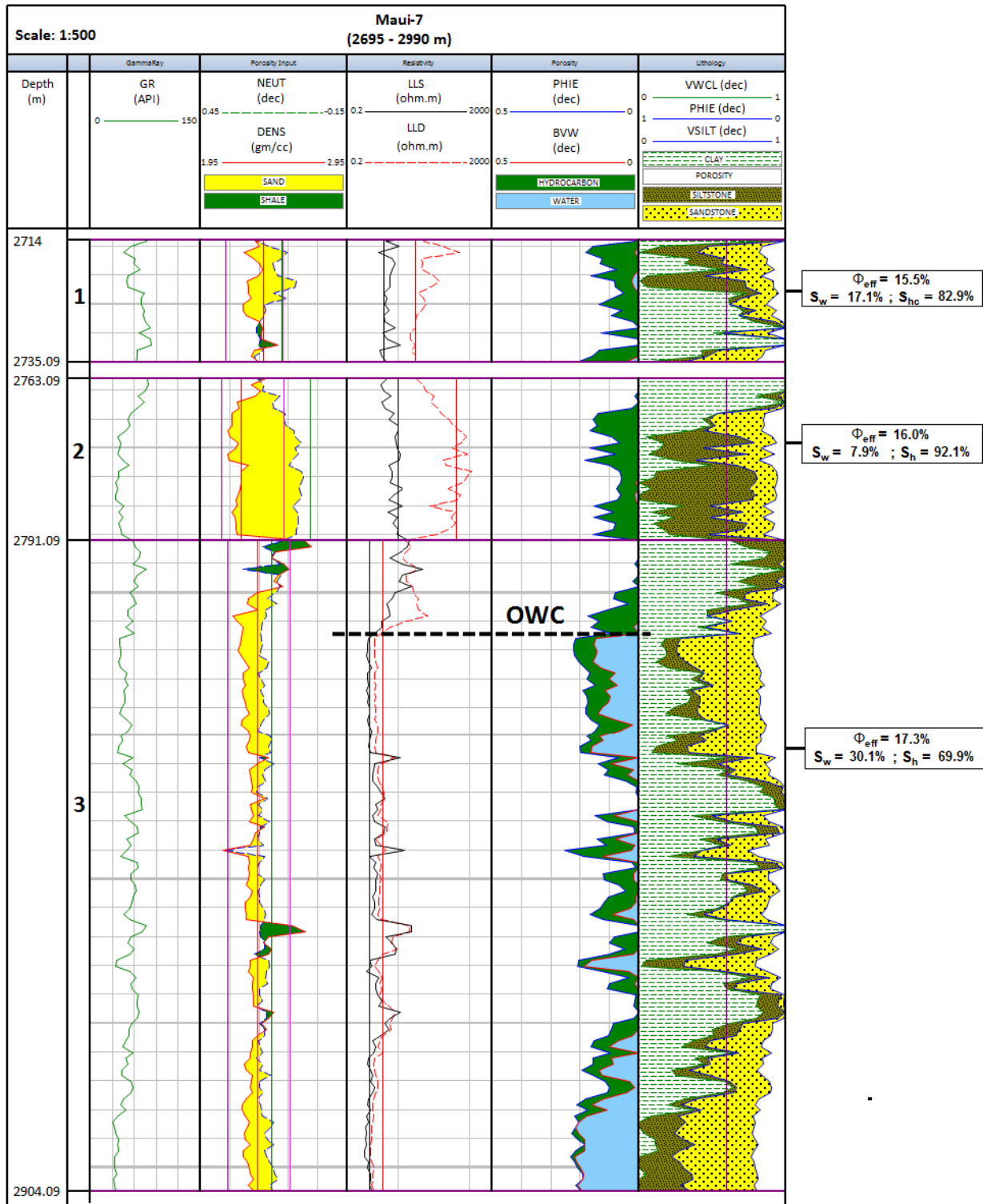


Figure 22. The interpreted well log data shows three promising pay zones, with Zone 2 being the most promising in the Maui 7 Well.

1D basin modeling has been performed on the data collected from the Cardiff-1 Well (see **Figure 23**), and a simplified petroleum system event chart has been built in **Figure 26** to show the general temporal relations among the essential petroleum system elements and processes in this study. During the Lower Miocene (18.8 Ma ago) the Mangahewa source rocks started generating oil in at 2900m depth with a TR% of 22mgHC/gTOC. Furthermore, a

TR% of 10 mgHC/gTOC is predicted for gas generation, which started during the Middle Miocene (16.2 Ma ago at a depth approximately of 3220 m). It appears also that the postmature condensate zone has been reached at 4920m depth at 3.7 Ma ago. In addition, it is observed that the Mangahewa Formation has not yet achieved peak generation, as hydrocarbons are continually undergoing expulsion in the present day.

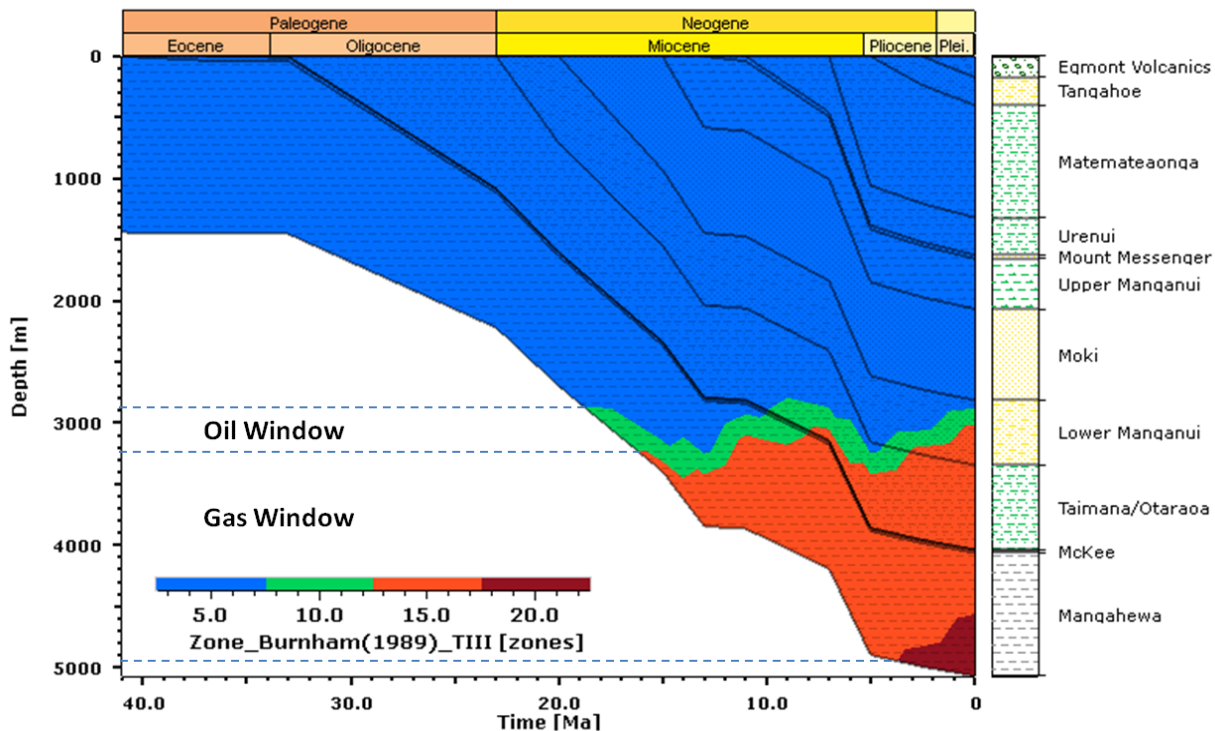


Figure 23. 1D basin modeling and the timing of hydrocarbon generation in the Cardiff-1 Well in the Mangahewa Formation.

Therefore, hydrocarbon production began during the Lower Miocene in the mature source rocks of the Mangahewa Formation, which are organic-rich coals, shaly coal, shale, and mudstones. Once a sufficient quantity and maturity has been attained, these hydrocarbons are expelled and migrate into the more porous and permeable reservoir zones of the same formation. The mudstones of the Turi Formation act as the cap rocks, whereas overburden rocks include all the overlying strata. The hydrocarbons most likely migrate upwards stratigraphically and structurally through the beds. This generation, migration, and accumulation are expected to be continuing to the

present day as more source rock units are expected to achieve sufficient maturity.

5. Conclusion

A comprehensive study of characteristics of the petroleum system in the Mangahewa Formation has been conducted. The variable lithologies of the Mangahewa Formation, ranging from sandstone, siltstone and mudstone to bituminous coal, contribute to the formation being both an excellent potential source and reservoir rock.

The study was conducted by integrating geochemical data, which encompasses Rock-Eval

pyrolysis, organic petrographical data and geochemical biomarkers, with petrophysical assessment, thin section petrographic description, well logging interpretation and 1D basin modeling.

The results show that the Mangahewa Formation has good source rock potential, with a TOC content of up to 90 wt. % and pyrolysis S_2 yields reaching 280 mg HC/g rock. The source rock organic matter is classified mostly as kerogen

type II-III, type II and type III which can generate oil and/or gas. Coal and shaly coal samples show the predominance of vitrinite macerals, probably perhydrous, whereas the shale samples are rich in liptinite, and /or migrabitumens. The maturity of the samples ranges between immature and mature, based collectively on the pyrolysis parameter T_{max} , the vitrinite reflectance, and biomarker maturity indicators.

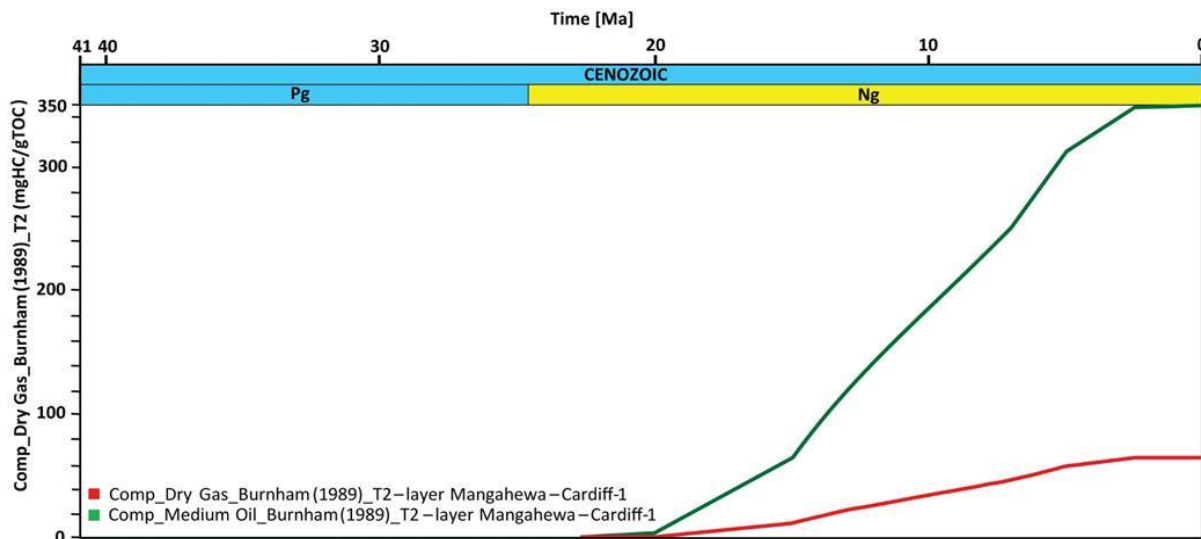


Figure 24. Source rock transformation ratio in the Cardiff-1 Well in the Mangahewa Formation.

The Mangahewa Formation also possesses good reservoir quality, based on petrographical, sedimentological, and petrophysical analyses. Diagenetic features such as compaction, cementation, clay authigenesis, and dissolution are observed, with porosity being the most dominant. As a result, abundant porosity has a significant part in producing good reservoir quality. As a whole, the porosity and permeability values are classified as good, with a positive correlation as permeability values increase with increasing porosity. All of these findings are further supported by promising well log evaluation results, which indicate that the Mangahewa Formation has an average effective porosity of 15.7%, with 32.1% average water saturation.

It is also proposed that the formation is sealed by the mudstones of the overlying Turi Formation,

which acts as the caprock. The trapping mechanism can be considered to include both structural and stratigraphic traps. The expulsion of hydrocarbons began during the Miocene and this expulsion, migration, and accumulation are expected to continue to the present day as the source rock attains more maturity. The results from this comprehensive study demonstrate that the Middle to Late Eocene Mangahewa Formation can be satisfactorily considered as a complete petroleum system unit.

Highlights

- The Mangahewa Formation has excellent organic matter and generation potential.
- The Mangahewa Formation has good porosity and permeability as a reservoir rock.
- The Mangahewa Formation is considered to be a complete petroleum system.

- Stratigraphic and structural traps are common features of the hydrocarbon accumulations.

Acknowledgements

The authors are grateful to New Zealand Petroleum and Minerals, of the Ministry of Business, Innovation and Employment (MBIE), for providing the data and rock samples, as well as giving approval for the re-evaluation,

interpretation, and publication of the dataset. Special thanks go to Mr. Ian Della Torre and Mr. Daniel Willmott for their technical assistance during the research trip to New Zealand and to AKM Ehsanul Haque for carrying the rock samples to Brunei Darussalam. Last but not least, sincere gratitude is also extended to Universiti Brunei Darussalam for providing assistance and support in completing this research.

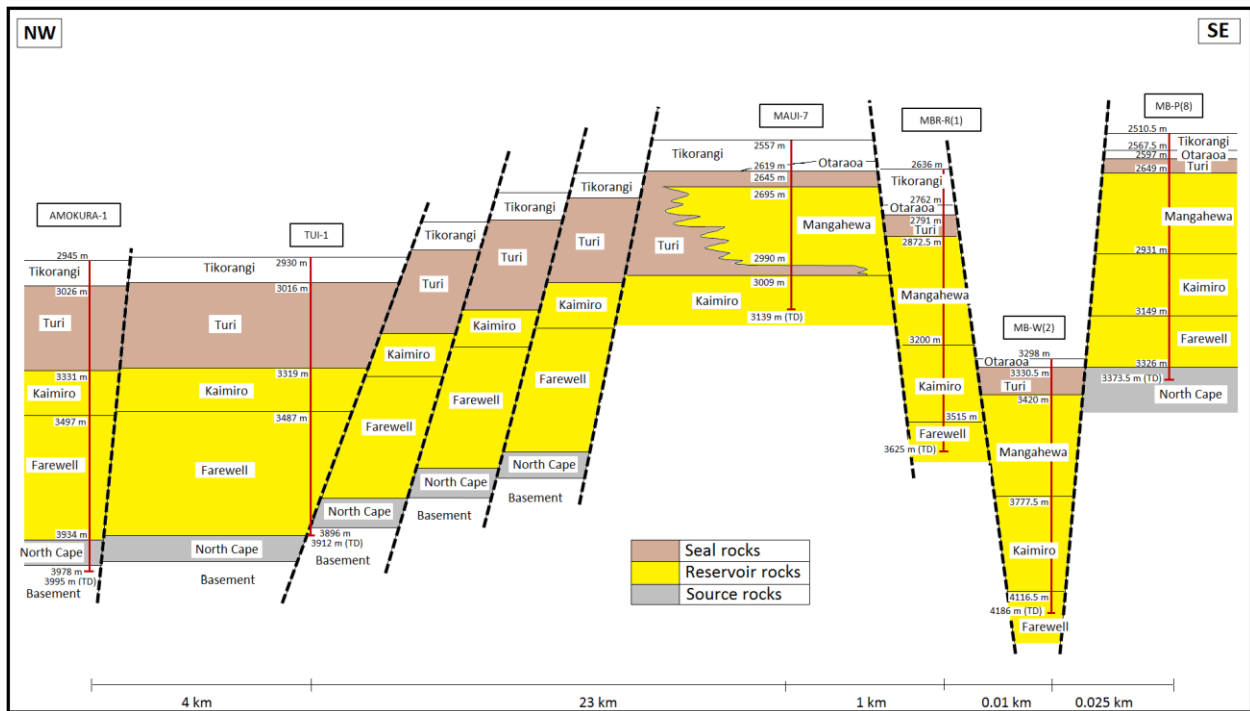


Figure 25. Hypothetical subsurface sketch showing the petroleum system elements and simplified subsurface structural configurations, based on the well log data.⁷⁶

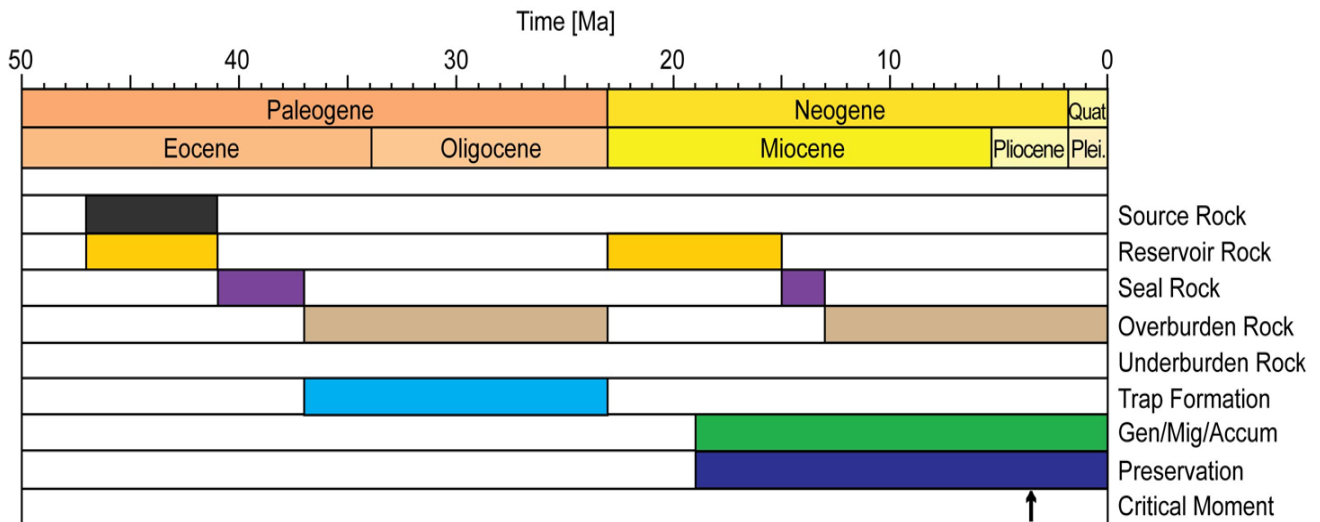


Figure 26. Petroleum system event chart showing the expected complete petroleum system elements and processes for the Mangahewa Formation.

References

- [1] New Zealand Petroleum and Minerals. *New Zealand Petroleum Basins 2014/2015 Revised Edition*, p. 105, Ministry of Business, Innovation and Employment, New Zealand, Wellington, 2014.
- [2] B. P. Tissot and D. H. Welte, D. H., *Petroleum Formation and Occurrence (2nd Edition)*, Springer Verlag, Berlin, 1984.
- [3] K. E. Peters and M. R. Cassa, "Applied source rock geochemistry" in L. B. Magoon and W. G. Dow (eds.), *The petroleum system – from source to trap*, American Association of Petroleum Geologists Memoir, 60, 93-120, 1994.
- [4] R. J. Collier and J. H. Johnston, "The identification of possible hydrocarbon source rocks, using biomarker geochemistry in the Taranaki Basin, New Zealand," *Journal of Southeast Asian Earth Sciences*, 5, 231-239, 1991.
- [5] S. D. Killips and N. L. Frewin, "Triterenoid diagenesis and cuticular preservation," *Organic Geochemistry*, 21, 1193-1209, 1994.
- [6] A. P. Murray *et al.*, "Biomarker and n-alkane isotope profiles for Tertiary oils: relationship to source rock depositional setting," *Organic Geochemistry*, 22, 521, 1994.
- [7] S. D. Killips *et al.*, "Predicting generation and expulsion of paraffinic oil from vitrinite-rich coals" *Organic Geochemistry*, 29, 1-21, 1998.
- [8] R. Sykes and L. R. Snowden, "Guidelines for assessing the petroleum potential of coaly source rocks using Rock-Eval pyrolysis," *Organic Geochemistry*, 33, 1441-1455, 2002.
- [9] R. W. Wilkins and S. C. George, "Coal as a source rock for oil: a review," *International Journal of Coal Geology*, 50, 317-361, 2002.
- [10] R. Sykes *et al.*, "Marine influence helps preserve the oil potential of coaly source rocks: Eocene Mangahewa Formation, Taranaki Basin, New Zealand," *Organic Geochemistry*, 66, 140-163, 2014.
- [11] S. Qadri *et al.*, "Source rock characterization and hydrocarbon generation modelling of the middle to late Eocene Mangahewa Formation in Taranaki Basin, New Zealand," *Arabian Journal of Earth Sciences*, 9, 559, 2016.
- [12] N. Jumat, M. R. Shalaby and M. A. Islam, "An integrated source rock characterization using geochemical analysis and well logs: a case study of Taranaki Basin, New Zealand," *Petroleum and Coal*, 59, 884-910, 2017.
- [13] S. Kalaitzidis *et al.*, "Late Cretaceous coal overlying karstic bauxite deposits in the Parnassus-Ghiona Unit, Central Greece: Coal characteristics and depositional environment," *International International Journal of Coal Geology*, 81, 211-226, 2010.
- [14] R. Kara-Gülbay *et al.*, "Source rock potential and organic geochemistry of Cenomanian-Turonian black shales, Western Taurus, SW Turkey," *Journal of Petroleum Geology*, 33, 355-369, 2010.
- [15] M. R. Shalaby, H. M. Hakimi and W. H. Abdullah, "Geochemical characteristics and hydrocarbon generation modeling of the Jurassic source rocks in the Shoushan Basin, north Western Desert, Egypt," *Marine and Petroleum Geology*, 28, 1611-1624, 2011.
- [16] M. R. Shalaby, H. M. Hakimi and W. H. Abdullah, "Modeling of gas generation from the Alam El-Bueib formation in the Shoushan Basin, northern Western Desert of Egypt," *Int. J. Earth Sci.*, 102, 319-332, 2012.
- [17] M. R. Shalaby, H. M. Hakimi and W. H. Abdullah, "Organic geochemical characteristics and interpreted depositional environment of the Khatatba Formation, northern Western Desert, Egypt," *AAPG Bulletin*, 96, 2019-2036, 2012.
- [18] M. R. Shalaby, H. M. Hakimi and W. H. Abdullah, "Geochemical characterization of solid bitumen (migrabitumen) in the Jurassic sandstone reservoir of the Tut

- Field, Shushan Basin, northern Western Desert of Egypt,” *International Journal of Coal Geology*, 100, 26-39, 2012.
- [19] M. R. Shalaby *et al.*, “Integrated TOC prediction and source rock characterization using machine learning, well logs and geochemical analysis: Case study from the Jurassic source rocks in Shams Field, NW Desert, Egypt,” *Journal of Petroleum Science and Engineering*, 176, 369-380, 2019.
- [20] M. R. Shalaby *et al.*, “Thermal maturity and depositional palaeoenvironments of the Cretaceous-Palaeocene Source Rock Taratu Formation, Great South Basin, New Zealand,” *Journal of Petroleum Sciences and Engineering*, 181, 106156, 2019.
- [21] M. R. Shalaby *et al.*, “Thermal maturity and TOC prediction using machine learning techniques: case study from the Cretaceous–Paleocene source rock, Taranaki Basin, New Zealand,” *J. Petrol Explor. Prod. Technol.*, 10, 2175-2193, 2020.
- [22] N. Jumat *et al.*, “Geochemical characteristics, depositional environment and hydrocarbon generation modeling of the upper cretaceous Pakawau group in Taranaki Basin, New Zealand,” *J. Pet. Sci. Eng.*, 163, 320-329, 2018.
- [23] L. N. Osli, M. R. Shalaby and M. A. Islam, “Characterization of source rocks and depositional environment, and hydrocarbon generation modelling of the cretaceous Hoiho Formation, Great South Basin, New Zealand,” *Petroleum and Coal*, 60, 255-275, 2018.
- [24] L. N. Osli, M. R. Shalaby and M. A. Islam, “Hydrocarbon generation modeling and source rock characterization of the Cretaceous-Paleocene Taratu Formation, Great South Basin, New Zealand,” *Journal of Petroleum Exploration and Production Technology*, 9, 125-139, 2019.
- [25] N. Jumat, M. R. Shalaby and M. A. Islam, “Integrated reservoir characterization of the Paleocene Farewell Formation, Taranaki Basin, New Zealand, using petrophysical and petrographical analyses,” *Journal of Petroleum Exploration and Production Technology (PEPT)*, 8, 685-701, 2018.
- [26] S. P. Dong, M. R. Shalaby and M. A. Islam, “Integrated reservoir characterization study of the McKee Formation, Onshore Taranaki Basin,” *New Zealand Geosciences*, 8, 105, 2018.
- [27] M. R. Shalaby, H. M. Hakimi and W. H. Abdullah, “Petroleum system analysis of the Khatatba formation in the Shoushan basin, north western desert, Egypt,” *Arabian Journal of Geosciences*, 7, 4303-4320, 2014.
- [28] M. R. Shalaby *et al.*, “Implications of controlling factors in evolving reservoir quality of the Khatatba Formation, Western Desert, Egypt,” *Scientia Bruneiana Special Issue*, 129-146, 2016.
- [29] L. N. Osli *et al.*, “Log-based petrophysical analysis of Khatatba Formation in Shoushan Basin, North Western Desert, Egypt,” *Geoscience Journal (GJ)*, The Association of Korean Geoscience Societies and Springer, 2018.
- [30] G. P. Thrasher, “Last Cretaceous Geology of Taranaki Basin, New Zealand,” PhD thesis, Victoria University of Wellington, Research Archive, 1992.
- [31] P. R. King and G. P. Thrasher, *Cretaceous-cenozoic Geology and Petroleum Systems of The Taranaki Basin, New Zealand*, Institute of Geological & Nuclear Sciences monograph, p. 13, 1996.
- [32] J. Palmer and G. Bulte, “Taranaki Basin, New Zealand,” in K. T. Biddle (Ed.) *Active Margin Basins*, 269-290, 1991.
- [33] J. Palmer, “Pre-miocene lithostratigraphy of Taranaki Basin, New Zealand,” *New Zealand Journal of Geology and Geophysics*, 28, 197–216, 1985.
- [34] C. Uruski, “Deepwater Taranaki, New Zealand: structural development and petroleum potential,” *Exploration Geophysics*, 39, 94-107, 2008.
- [35] W. F. H. Pilaar and L. L. Wakefield, “Structural and stratigraphic evolution of the Taranaki Basin, offshore North Island, New Zealand,” *APPEA Journal of*

- Australian Petroleum Production and Exploration Association*, 18, 93-101, 1978.
- [36] J. Baur, R. Sutherland and T. Stern, "Anomalous passive subsidence of deep-water sedimentary basins: a prearc basin example, southern New Caledonia Trough and Taranaki Basin, New Zealand," *Basin Research*, 26, 242-268, 2014.
- [37] K. Kroeger *et al.*, "3D crustal scale heat-flow regimes at a developing active margin (Taranaki Basin, New Zealand)," *Tectonophysics*, 591, 175-193, 2013.
- [38] P. A. Armstrong *et al.*, "Thermal modelling and hydrocarbon generation in an active-margin basin: Taranaki Basin, New Zealand," *American Association of Petroleum Geologists Bulletin*, 80, 1216-1241, 1996.
- [39] International Organization for Standardization (ISO). *Methods for the petrographic analysis of bituminous coal and anthracite — Part 2: Method for preparing coal samples*, Geneva, Switzerland, 7404-2, 2014.
- [40] American Standard for Testing and Materials (ASTM). *Standard test method for microscopical determination of the reflectance of vitrinite dispersed in sedimentary rocks*, D7708, 2014.
- [41] International Committee for Coal and Organic Petrology (ICCP). "The new vitrinite classification (ICCP System 1994)," *Fuel*, 77, 349-358, 1998.
- [42] International Committee for Coal and Organic Petrology (ICCP). "The new inertinite classification (ICCP System 1994)," *Fuel*, 80, 459-471, 2001.
- [43] I. Sýkorová *et al.*, "Classification of huminite – ICCP System 1994," *International Journal of Coal Geology*, 62, 85-106, 2005.
- [44] W. Pickel *et al.*, "Classification of liptinite – ICCP System 1994," *International Journal of Coal Geology*, 169, 40-61, 2017.
- [45] C. R. Landis and J. R. Castaño, "Maturation and bulk chemical properties of a suite of solid hydrocarbons," *Organic Geochemistry*, 22, 137-149, 1995.
- [46] H. Jacob, "Classification, structure, genesis and practical importance of natural solid bitumen ("migrabitumen")," *International Journal of Coal Geology*, 11, 65-79, 1989.
- [47] A. I. Levorsen, *Geology of Petroleum*, 2nd Edition, W. H. Freeman, San Francisco, 1967.
- [48] N. J. Godfrey *et al.*, "Crustal structure and thermal anomalies of the Dunedin region, South Island, New Zealand," *J. Geophys. Res. Solid Earth*, 106, 30835-30848, 2001.
- [49] A. Burnham, *A simple kinetic model of petroleum formation and cracking*, Lawrence Livermore National Lab., CA (USA), UCID-21665, 1989.
- [50] E. C. Bullard, "The time necessary for a bore hole to attain temperature equilibrium," *Geophys. J. Int.*, 5, 127-130, 1947.
- [51] D. W. Waples, and M. A. Ramly, "Simple statistical method for correcting and standardizing heat flows and subsurface temperatures derived from log and test data," *Bulletin of the Geological Society of Malaysia, Special Publication*, 37, 253-267, 1994.
- [52] D. W. Waples and M. A. Ramly, "Statistical method for correcting log-derived temperatures," *Pet. Geosci.*, 7, 231-240, 2001.
- [53] K. E. Peters and P. H. Nelson, "Criteria to determine borehole formation temperatures for calibration of basin and petroleum system models," in N. B. Harris and K. E. Peters (Eds.), *Analyzing the thermal history analysis of sedimentary basin: methods and case studies*, SEPM Special Publication, 5-16, 2012.
- [54] J. Espitalié *et al.*, "Methode rapide de caracterisation des roches meres de leur potential petrolier et de leur degre d'evolution," *Revue de l'Institut Francais du Petrole*, 32, 23-42, 1977.
- [55] G. H. Taylor *et al.*, *Organic Petrology*. Gebrüder Borntraeger, Berlin and Stuttgart, 704, 1998.
- [56] K. E. Peters, C. C. Walters and J. M. Moldowan, *The biomarker guide*, 2nd

- Edition*, Cambridge University Press, Cambridge, 2005.
- [57] N. D. Rodriguez and R. P. Philp, "Source rock facies distribution predicted from oil geochemistry in the Central Sumatra Basin, Indonesia," *AAPG Bulletin*, 99, 2005-2022, 2015.
- [58] J. M. Hunt, "Generation of gas and oil from coal and other terrestrial organic matter," *Organic Geochemistry*, 17, 673-680, 1991.
- [59] K. E. Peters and J. M. Moldowan, *The biomarker guide, interpreting molecular fossils in petroleum and ancient sediments*, Prentice Hall, New Jersey, 1993.
- [60] G. Rieley et al., "The biogeochemistry of Ellesmere Lake, UK I: source correlation of leaf wax inputs to the sedimentary record," *Organic Geochemistry*, 17, 901-912, 1991.
- [61] P. A. Meyers, "Application of organic geochemistry to paleolimnological reconstruction: a summary of examples from the Laurentian Great Lake," *Organic Geochemistry*, 34, 261-289, 2003.
- [62] F. R. Aquito Neto et al., "Occurrence and formation of tricyclic and tetracyclic terpanes in sediments and petroleum," in M. Bjoroy, P. Albrecht and C. Cornford (Eds.), *Advances in organic geochemistry 1981*, 659-667, John Wiley & Sons, New York, 1983.
- [63] C. Barker, "Pyrolysis techniques for source-rock evaluation," *American Association of Petroleum Geologists Bulletin*, 58, 2349-2361, 1974.
- [64] W. K. Seifert and J. M. Moldowan, "Use of biological biomarkers in petroleum exploration," in R. B. Johns (Ed.), *Methods in Geochemistry and Geophysics*, 24, 261-290, Elsevier, Amsterdam, 1986.
- [65] M. R. Shalaby et al., "Geochemical characteristics and depositional environments of the Narimba Formation source rock, Bass Basin, Australia," *Journal of Petroleum Exploration and Production Technology*, 10, 3207-3225, 2020.
- [66] R. G. Loucks, "Revisiting the importance of secondary dissolution pores in tertiary sandstones along the Texas Gulf Coast," *Gulf Coast Assoc. Geol. Soc.*, 55, 447-455, 2006.
- [67] M. R. Shalaby, M. H. Hakimi and W. H. Abdullah, "Diagenesis in the middle Jurassic Khatatba formation sandstones in the Shoushan basin, northern western desert, Egypt," *Geological Journal*, 49, 239-255, 2006.
- [68] M. R. Shalaby, S. H. Sapri and M. A. Islam, "Integrated reservoir characterization and fluid flow distribution of the Kaimiro Formation, Taranaki Basin, New Zealand," *Journal of Petroleum Exploration and Production Technology*, 10, 3263-3279, 2020.
- [69] M. A. K. El-ghali et al., "Distribution of diagenetic alterations in fluvial and paralic deposits within sequence stratigraphic framework: Evidence from the Petrohan Terrigenous Group and the Svidol Formation, Lower Triassic, NW Bulgaria," *Sedimentary*, 190, 299-321, 2006.
- [70] M. A. K. El-ghali et al., "Diagenetic alterations related to marine transgression and regression in fluvial and shallow marine sandstones of the Triassic Buntsandstein and Keupersequence, the Paris Basin, France," *Marine and Petroleum Geology*, 26, 289-309, 2009.
- [71] Schlumberger Educational Services, *Log interpretation principles*, Schlumberger, Houston, Texas, 1989.
- [72] M. Rider, *The geological interpretation of well logs (2nd edition)*, Whittles Publishing, London, 1996.
- [73] S. M. T. Qadri, M. A. Islam and M. R. Shalaby, "Three-Dimensional Petrophysical Modelling and Volumetric Analysis to Model the Reservoir Potential of the Kupe Field, Taranaki Basin, New Zealand," *Natural Resources Research*, 28, 369-392 (2019).
- [74] S. M. T. Qadri, M. A. Islam and M. R. Shalaby, "Application of well log analysis to estimate the petrophysical parameters and evaluate the reservoir

- quality of the Lower Goru Formation, Lower Indus Basin, Pakistan,” *Geomech. Geophys. Geo-energ. Georesour.*, 5, 271-288, 2019.
- [75] B. D. Field *et al.*, *An ArcGIS project on seal rocks of the New Zealand region*, GNS Science Consultancy Report 2014/232, 2014.
- [76] N. Jumat, “Integrated source and reservoir characterisation: Case study from the Cretaceous-Palaeogene formations, Taranaki Basin, New Zealand,” PhD Thesis, Universiti Brunei Darussalam, 2019.
- [77] W. Y. Huang and W. G. Meinschein, “Sterols as ecological indicators,” *Geochimica et Cosmochimica Acta*, 43, 739-745, 1979.

Table 1. Cutting samples from different wells in the Mangahewa Formation showing the bulk geochemical results of Rock-Eval and total organic carbon (TOC).

Well	Depth	Lithology	S1 (mg HC/g rock)	S2 (mg HC/g rock)	S3 (mg CO ₂ /g rock)	TOC (wt %)	HI (mg HC/g TOC)	OI (mg HC/g TOC)	PI	Tmax
Cardiff-1	4070	Coal	10.5	225	5.86	71.1	317	8.24	0.04	420
Cardiff-1	4080	Coal	10.1	217	6.37	72.4	299	8.80	0.04	419
Cardiff-1	4095	Coal	7.60	193	7.33	72.6	265	10.1	0.04	422
Cardiff-1	4095	Shaly coal	3.54	96.8	3.65	37.2	260	9.80	0.04	426
Cardiff-1	4095	Mudstone	0.64	20.6	1.06	8.3	248	12.7	0.03	431
Cardiff-1	4105	Coal	7.23	191	7.24	74.9	254	9.66	0.04	422
Cardiff-1	4145	Coal	6.24	185	7.22	76.3	242	9.46	0.03	427
Cardiff-1	4285	Coal	5.57	184	6.31	76.4	240	8.26	0.03	432
Cardiff-1	4660	Coal	15.7	208	3.42	79.4	262	4.31	0.07	443
Cardiff-1	4880	Coal	17.6	204	3.45	78.0	262	4.42	0.08	443
Cardiff-1	4880	Shaly coal	9.34	119	1.29	42.3	281	3.05	0.07	441
Cardiff-1	4880	Mudstone	1.08	8.20	1.54	5.07	162	30.4	0.12	436
Inglewood-1	3725	Coal	11.7	112	6.31	40.7	274	15.5	0.09	430
Inglewood-1	3755	Coal	10.6	103	7.22	26.0	397	27.8	0.09	433
Inglewood-1	3908	Coal	10.7	128	6.71	26.0	491	25.8	0.08	433
Inglewood-1	3968	Coal	12.8	148	10.5	45.1	328	23.3	0.08	436
Inglewood-1	4395	Coal	16.1	101	1.21	22.4	450	5.41	0.14	440
Inglewood-1	3801	Coal	8.84	181	7.56	68.1	266	11.1	0.05	428
Inglewood-1	3801	Mudstone	0.76	14.5	0.60	6.33	229	9.48	0.05	434
Inglewood-1	4334	Coal	12.8	189	5.31	67.5	280	7.87	0.06	434
Inglewood-1	4334	Mudstone	0.39	6.46	0.22	4.10	158	5.37	0.06	428
Kaimiro-1	3799	Coal	13.2	222	4.80	73.2	304	6.56	0.06	432
Kaimiro-1	3799	Shaly coal	5.78	77.1	2.84	33.6	229	8.44	0.07	432
Kaimiro-1	3799	Mudstone	1.95	28.4	1.04	10.9	260	9.53	0.06	431
Kaimiro-1	4030	Coal	13.9	231	4.68	75.7	305	6.19	0.06	432
Kaimiro-1	4030	Shaly coal	4.92	73.4	3.31	31.3	235	10.6	0.06	428
Kaimiro-1	4030	Mudstone	1.31	21.5	0.82	8.07	266	10.2	0.06	429
Kapuni-2	3292	Coal	4.90	49.7	8.00	30.6	162	26.1	0.09	432
Kapuni-2	3341	Coal	3.59	80.0	9.77	27.8	287	35.1	0.04	430
Kapuni-2	3511	Coal	16.5	166	13.4	53.5	311	25.0	0.09	432
Kapuni-2	3609	Shale	1.09	7.22	7.22	7.16	101	101	0.13	434
Kapuni-2	3731	Shale	0.63	2.34	2.34	3.68	64	63.6	0.21	433
Kapuni-2	3780	Coal	15.0	196	196	71.0	276	276	0.07	431
Kapuni-2	3804	Shale	3.29	39.4	39.38	18.4	214	214	0.08	434

Maui-4	2158	Coal	9.68	131	20.3	83.3	157	24.3	0.07	423
Maui-4	2158	Shaly coal	6.01	48.5	9.6	25.3	192	37.9	0.11	429
Maui-4	2158	Mudstone	2.41	18.2	3.4	8.36	217	40.7	0.12	425
Maui-4	2200	Coal	9.99	139	22.4	65.6	212	34.2	0.07	422
Maui-4	2200	Shaly coal	3.06	58.4	8.41	25.8	227	32.7	0.05	426
Maui-4	2200	Mudstone	0.70	12.0	2.08	5.56	215	37.4	0.06	422
Maui-5	2712	Shale	0.00	0.37	0.51	0.68	54	75.0	0.00	428
Maui-5	2800	Shale	0.56	12.0	1.71	6.74	178	25.4	0.04	429
Maui-6	2801	Shale	0.45	6.34	0.67	3.24	196	20.7	0.07	433
Maui-6	3027	Shale	0.11	3.01	0.37	2.69	112	13.8	0.04	428
Ngatoro-1	3997	Coal	8.72	207	7.07	74.9	276	9.44	0.04	431
Ngatoro-1	3997	Shaly coal	3.19	66.6	5.40	31.3	212	17.2	0.05	431
Ngatoro-1	3997	Mudstone	1.46	31.5	1.71	12.0	264	14.3	0.04	431
N- Tasman-1	2082	Coal	3.55	122	17.7	62.3	196	28.4	0.03	428
Ohanga-2	3969	Coal	26.0	277	1.50	74.7	371	2.01	0.09	419
Ohanga-2	3987	Coal	10.6	223	2.27	75.5	296	3.01	0.05	428
Ohanga-2	3990	Coal	10.1	234	1.78	77.4	303	2.30	0.04	433
Ohanga-2	4014	Coal	12.3	237	1.87	78.7	301	2.38	0.05	431
Ohanga-2	4019	Coal	13.1	270	2.66	90.0	300	2.95	0.05	431
Ohanga-2	4021	Shaly coal	7.73	280	0.67	65.6	427	1.02	0.03	430
Ohanga-2	4140	Coal	18.1	250	1.11	69.3	360	1.60	0.07	428
Ohanga-2	4140	Coal	22.6	253	1.89	74.2	341	2.55	0.08	429
Ohanga-2	4144	Coal	10.9	214	2.06	77.1	277	2.67	0.05	433
Ohanga-2	4173	Coal	13.4	234	1.58	77.7	301	2.03	0.05	435
Ohanga-2	4182	Coal	16.4	244	1.43	73.5	332	1.94	0.06	433
Ohanga-2	4224	Coal	13.5	224	2.46	74.3	302	3.31	0.06	434
Ohanga-2	4299	Coal	13.6	224	2.34	76.3	293	3.07	0.06	437
Ohanga-2	4308	Coal	14.8	225	2.59	76.1	296	3.40	0.06	436
Ohanga-2	4317	Coal	12.2	226	1.81	77.5	292	2.34	0.05	437
Ohanga-2	4353	Coal	14.2	215	1.98	77.3	278	2.56	0.06	437
Okoki-1	3870	Mudstone	0.15	1.53	0.67	1.17	131	57.3	0.09	441
Okoki-1	4155	Mudstone	0.19	1.62	0.47	1.21	134	38.8	0.10	443
Okoki-1	4185	Mudstone	0.37	2.61	1.09	2.06	127	52.9	0.12	442
Okoki-1	4215	Mudstone	0.24	1.93	0.35	1.36	142	25.7	0.11	445
Pukeko-1	3355	Coal	8.99	193	3.20	57.4	337	5.58	0.04	414
Pukeko-1	3415	Coal	11.4	169	2.96	47.5	356	6.23	0.06	419
Pukeko-1	3425	Coal	10.1	149	3.06	44.2	337	6.92	0.06	416
Urenui-1	3508	Shale	0.51	3.69	0.55	1.90	194	28.9	0.12	430
Urenui-1	3569	Coal	1.81	21.1	0.98	7.02	301	14.0	0.08	433
Urenui-1	3600	Coal	5.60	67.8	3.26	20.2	335	16.1	0.08	437

Urenui-1	3752	Coal	9.31	120	3.87	37.0	325	10.5	0.07	440
Waihapa-1	4026	Coal	11.1	238	4.64	73.7	322	6.29	0.04	425
Waihapa-1	4050	Coal	6.95	205	5.11	73.2	280	6.98	0.03	428
Waihapa-1	4110	Coal	7.00	177	7.30	75.6	234	9.66	0.04	430
Waihapa-1	4182	Coal	5.63	182	7.03	75.0	243	9.38	0.03	433
Waihapa-1	4218	Coal	8.30	198	6.19	73.9	268	8.38	0.04	430
Waihapa-1	4257	Coal	7.52	171	7.52	74.4	230	10.1	0.04	432
Waihapa-1	4293	Coal	6.48	158	7.01	76.4	207	9.17	0.04	437
Waihapa-1	4299	Coal	5.93	157	7.29	75.5	208	9.66	0.04	438
Waihapa-1A	4674	Coal	6.62	155	4.87	73.2	212	6.65	0.04	440
Waihapa-1A	4674	Shaly coal	2.86	81.0	2.75	33.7	241	8.17	0.03	443
Waihapa-1A	4674	Mudstone	0.90	23.2	0.63	8.86	262	7.11	0.04	442
Waihapa-1A	4719	Coal	12.1	201	4.07	80.9	248	5.03	0.06	447

Table 2. List of samples assessed for thermal maturity using T_{max} and vitrinite reflectance (VR%).

Well	Depth	Lithology	Tmax (C)	VR (%)
Cardiff-1	4070	Coal	420	0.61
Cardiff-1	4080	Coal	419	0.63
Cardiff-1	4095	Coal	422	0.69
Cardiff-1	4105	Coal	422	0.7
Cardiff-1	4145	Coal	427	0.72
Cardiff-1	4285	Coal	432	0.72
Cardiff-1	4660	Coal	443	0.87
Inglewood-1	4395	Coal	440	0.72
Kapuni-2	3780	Coal	431	0.61
Ohanga-2	3969	Coal	419	0.51
Ohanga-2	3987	Coal	428	0.77
Ohanga-2	3990	Coal	433	0.75
Ohanga-2	4014	Coal	431	0.69
Ohanga-2	4140	Coal	428	0.56
Ohanga-2	4140	Coal	429	0.6
Ohanga-2	4144	Coal	433	0.76
Ohanga-2	4173	Coal	435	0.73
Ohanga-2	4182	Coal	433	0.67
Ohanga-2	4224	Coal	434	0.71
Ohanga-2	4299	Coal	437	0.78
Ohanga-2	4308	Coal	436	0.75
Ohanga-2	4317	Coal	437	0.75
Ohanga-2	4353	Coal	437	0.8
Pukeko-1	3355	Coal	414	0.53
Urenui-1	3569	Coal	433	0.63
Urenui-1	3752	Coal	440	0.76
Waihapa-1	4026	Coal	425	0.55
Waihapa-1	4050	Coal	428	0.59
Waihapa-1	4110	Coal	430	0.69
Waihapa-1	4182	Coal	433	0.69
Waihapa-1	4218	Coal	430	0.66
Waihapa-1	4257	Coal	432	0.71
Waihapa-1	4293	Coal	437	0.75
Waihapa-1	4299	Coal	438	0.77
Toko-1	4173	Coal	428	0.66
Toko-1	4216	Coal	427	0.63
Toko-1	4231	Coal	434	0.74

Table 3. Maceral compositions of Mangahewa coal samples.

Well	Depth	Lithology	Amorphous + Alginite + Liptinite (%)	Vitrinite (%)	Inertinite (%)
Cardiff-1	4070	Coal	7.4	87.6	5
Cardiff-1	4080	Coal	4.5	86.8	8.7
Cardiff-1	4095	Coal	7	87.6	5.4
Cardiff-1	4105	Coal	8.5	85	6.5
Cardiff-1	4145	Coal	4.8	85.9	9.3
Cardiff-1	4285	Coal	7.3	87.5	5.2
Inglewood-1	4395	Coal	13.4	79.7	6.9
Kapuni-2	3780	Coal	8.9	88.9	2.21
Urenui-1	3569	Coal	19	65	16
Urenui-1	3752	Coal	18	71	12
Waihapa-1	4026	Coal	10.7	84.7	4.6
Waihapa-1	4050	Coal	9.6	80.7	9.7
Waihapa-1	4110	Coal	7.2	88.4	4.4
Waihapa-1	4182	Coal	4	85.9	10.1
Waihapa-1	4218	Coal	4.2	83.3	12.5
Waihapa-1	4257	Coal	4.1	85.4	10.5
Waihapa-1	4293	Coal	2	90.7	7.3
Waihapa-1	4299	Coal	2	88.3	9.7
Toko-1	4173	Coal	7.7	80.6	11.7
Toko-1	4216	Coal	5.7	82.2	12.1
Toko-1	4231	Coal	6.8	86.4	6.8
Toko-1	4321	Coal	4.9	82.9	12.2
Mangahewa-2	3539	Coal	3.3	83.8	12.9
Mangahewa-2	3552	Coal	13.4	82.1	4.5
Mangahewa-2	3557	Coal	14.1	77.8	8.1
Mangahewa-2	3576	Coal	4.4	92.3	3.3
Mangahewa-2	3583	Coal	14.1	83	2.9
Mangahewa-2	3717	Coal	6.6	88.1	5.3
Mangahewa-2	3725	Coal	5.7	83.3	11
Mangahewa-2	3784	Coal	4.9	89	6.1
Mangahewa-2	3789	Coal	6.1	87.7	6.2
Mangahewa-2	3815	Coal	3.2	85.1	11.7
Mangahewa-2	3840	Coal	5.4	87.2	7.4
Mangahewa-2	3849	Coal	4.8	88.7	6.5
Mangahewa-2	3867	Coal	6.8	85.6	7.6
Mangahewa-2	3895	Coal	15.3	83.1	1.6
Mangahewa-2	3915	Coal	7.7	85.5	6.8

Table 4. Biomarker parameters calculated from n-alkanes and isoprenoids.

Well	Pr/Ph	Pr/nC ₁₇	Ph/nC ₁₈	CPI	OEP	TAR	Waxiness
Maui-4	2.74	0.5	0.19	1.23	1.23	0.17	0.46
	2.68	0.48	0.15	1.06	1.07	0.09	0.46
	3.18	0.46	0.16	1.14	1.13	0.14	0.5
	9.39	1.79	0.28	1.51	1.05	0.91	1.29
	6.37	1.13	0.21	1.51	1.15	0.56	1.08
	8.39	2.88	0.32	1.5	1.15	1.29	2.3
	8.24	3.4	0.36	1.56	1.16	1.69	2.85
	3.97	0.67	0.14	1.23	1.1	0.27	0.73
	6.95	4.86	0.75	1.2	1.02	0.79	1.54
	9.08	2.43	0.26	1.44	1.19	1.65	2.79
	9.54	4.37	0.37	1.5	1.23	2.5	4.05
6.59	1.17	0.16	1.11	1.07	0.38	1.26	
Maui-5	5.08	2.47	0.64	1.58	1.07	2.39	1.95
	13.35	4.16	0.39	1.59	1.18	1.42	1.67
Maui-6	12.38	11.61	0.85	1.79	1.16	11.55	9.06
	11.02	14.11	1.05	1.53	1.13	5.41	4.94
Okoki-1	4.64	3.5	0.7	1.2	1.06	1.89	2.6
	4.97	2.67	0.56	1.13	1.05	1.65	2.51
	5.04	2.3	0.49	1.14	1.05	1.71	2.63
	5.07	2.47	0.48	1.13	1.04	1.92	2.85
Waihapa-1	8.6	7.21	0.81	1.34	1.26	1.74	3.1
	10.77	3.95	0.33	1.21	1.11	1.26	2.23
Waihapa-1A	7.06	1.38	0.2	1.11	1.07	0.83	1.65
	5.36	0.79	0.15	1.09	1.03	0.65	1.39
	4.43	0.89	0.19	1.08	0.99	1.1	2.05
	8.56	1.54	0.17	1.1	1.05	0.6	1.51
Toko-1	8.85	3.55	0.38	1.17	1.17	0.71	1.39
	12.38	3.51	0.26	1.17	1.04	0.76	1.77
	9.81	3.15	0.29	1.1	1.01	1.02	2.22
	5.06	0.84	0.15	1.14	1.21	0.3	0.95
Kaimir 0-1	13.23	6.79	0.41	1.29	1.1	1.85	2.76
	12.32	5.84	0.42	1.25	1.08	1.45	2.32

	2.88	0.66	0.24	1.05	1.03	0.21	0.71
	3.34	1.11	0.31	1.06	1.06	0.21	1.04
	3.12	1.18	0.32	1.08	1.02	0.89	1.76
Ohanga-2	10.35	7.09	0.57	1.11	1.02	1.46	2.87
	6.6	6.4	0.82	1.09	1.01	2.49	4.23
	6.26	6.21	0.83	1.1	1.02	2.17	3.76
	4.71	2.73	0.51	1.01	1.04	0.59	1.32
	10.04	9.54	0.86	1.16	1.02	2.94	4.64
	7.73	8.62	0.87	1.16	1.02	2.45	3.85
	7.16	7.08	0.84	1.15	1.05	2.34	3.67
Pukeko-1	8.06	12.69	3.4	1.43	0.94	3.27	4.93
	10.98	5.22	0.83	1.59	1.12	2.47	3.68
	8.72	5.89	1.22	1.26	1.07	1.1	2.25
	8.12	15.51	2.6	1.26	0.92	1.68	3.34

Table 5. Biomarker parameters calculated from hopanes and terpanes.

Well	19tri/23tri	24tri/23tri	C ₃₂ S/S+R	G
Maui-5	-	-	0.27	0.00
	0.67	0.62	0.33	0.00
Maui-6	-	-	0.40	0.00
	0.80	0.83	0.47	0.00
Okoki-1	0.10	0.45	0.58	0.07
	1.26	0.54	0.59	0.03
	0.95	0.49	0.59	0.04
	1.63	0.56	0.58	0.03
Waihapa-1	1.63	1.54	0.61	0.02
	8.82	2.00	0.61	0.01
Waihapa-1A	9.55	0.48	0.60	0.02
	3.51	0.46	0.59	0.02
	2.26	0.48	0.59	0.03
	22.50	0.68	0.60	0.02
Toko-1	10.02	1.21	0.61	0.02
	18.92	1.30	0.59	0.02
	23.29	0.83	0.60	0.02
	23.13	0.55	0.57	0.05
Kaimiro-1	12.37	4.10	0.60	0.02
	9.69	2.89	0.60	0.02
	1.21	0.41	0.59	0.03
	0.65	0.42	0.59	0.03
	0.57	0.44	0.58	0.04
Ohanga-2	11.00	0.31	0.59	0.01
	8.04	0.36	0.59	0.01
	9.81	0.36	0.60	0.01
	4.51	0.43	0.58	0.01
	9.38	0.40	0.60	0.01
	10.88	0.33	0.60	0.01
	9.56	0.00	0.59	0.01
u i	2.66	0.53	0.23	0.02

	2.04	0.55	0.29	0.02
	2.32	0.47	0.28	0.03
	3.21	3.23	0.32	0.02
	2.20	0.65	0.39	0.02
	2.85	0.94	0.38	0.01
	3.64	0.71	0.40	0.02
	4.43	0.00	0.51	0.02
	3.08	0.73	0.59	0.02
	6.57	0.71	0.59	0.02
	6.47	0.60	0.59	0.02
	17.88	0.60	0.61	0.01
Pukeko-1	31.82	0.69	0.48	0.02
	17.48	0.63	0.57	0.01
	98.31	0.61	0.53	0.02
	-	-	0.53	0.01

Table 6. Biomarker parameters calculated from steranes.

Well	%C ₂₇	%C ₂₈	%C ₂₉	C ₂₉ S/(S+R)	C ₂₉ ββ/(αα+ ββ)
Maui-5	29.49	0.00	70.51	0.00	0.00
	18.48	22.01	59.51	0.20	0.33
Maui-6	14.92	11.99	73.09	0.14	0.33
	23.04	0.00	76.96	0.20	0.39
Okoki-1	35.70	21.01	43.29	0.53	0.48
	31.57	16.72	51.71	0.58	0.50
	28.42	16.76	54.81	0.54	0.53
	28.85	16.39	54.75	0.59	0.49
Waihapa-1	8.93	14.36	76.71	0.50	0.35
	5.71	13.03	81.26	0.50	0.28
Waihapa-1A	0.00	15.41	84.59	0.52	0.52
	19.03	18.58	62.39	0.57	0.54
	26.66	18.29	55.04	0.59	0.53
	8.94	17.01	74.05	0.55	0.52
Toko-1	7.84	12.97	79.19	0.51	0.46
	0.00	12.35	87.65	0.50	0.38
	0.00	14.42	85.58	0.55	0.50
	19.41	13.95	66.64	0.63	0.50
Kaimiro-1	8.77	16.49	74.74	0.51	0.34
	8.92	15.12	75.95	0.51	0.35
	33.79	21.44	44.76	0.58	0.55
	38.36	17.90	43.73	0.63	0.56
	38.65	19.69	41.66	0.62	0.57
Ohanga-2	7.52	9.30	73.17	0.45	0.39
	7.51	17.48	75.01	0.49	0.50
	6.11	18.44	75.44	0.48	0.49
	7.85	16.00	76.15	0.50	0.45
	12.47	19.04	68.49	0.50	0.51
	7.87	17.48	74.65	0.47	0.49
	10.89	18.35	70.76	0.48	0.53
Maui-4	9.78	16.89	73.33	0.18	0.34
	13.59	18.58	67.83	0.22	0.40
	12.33	17.24	70.42	0.25	0.38
	5.06	13.16	81.78	0.12	0.24
	3.74	20.54	75.73	0.15	0.18
	3.09	19.76	77.15	0.14	0.17
	2.32	23.97	73.72	0.14	0.20

	6.38	14.02	79.60	0.25	0.34
	6.71	12.10	81.19	0.46	0.30
	3.94	11.37	84.69	0.47	0.20
	4.79	13.50	81.71	0.49	0.22
	0.00	14.31	85.69	0.53	0.52
Pukeko-1	6.04	16.82	77.14	0.22	0.34
	5.21	40.00	54.79	0.28	0.52
	0.00	0.00	100.00	0.21	0.43
	0.00	11.46	88.54	0.30	0.36

Table 7. Petrophysical data for selected sandstone core samples from the Mangahewa Formation.

Well	Depth (m)	Porosity (%)	Permeability (mD)
Maui-5	2807	21.6	5900.0
Maui-5	2852	18.8	1800.0
Maui-6	2789	20.7	6900.0
Maui-6	2821	24.9	210.0
Maui-6	2862	21.1	5800.0
MB-P(8)	2970	21.4	105.9
MB-P(8)	2973	24.6	5403.0
Moki-1	2092	17.40	92.0
Moki-1	2094	15.60	22.0
Moki-1	2096	17.40	275.0
Moki-1	2103	17.00	111.0
Moki-1	2112	18.40	25.0
Moki-1	2125	11.50	7.1
Moki-1	2129	9.50	1.2
Moki-1	2131	13.40	6.9
Moki-1	2131	17.50	203.0

Table 8. Well log petrophysical report of sandstone reservoir zones in the Mangahewa Formation.

Well	Thickness/Net (m)					Porosity (%)			Fluids (%)	
	Top	Bottom	Thick-ness	Net Res	Net Pay	PHIT	PHIE	V _{cl}	S _w	S _h
Maui-7	2695	2990	295	78.5	19.5	25.0%	16.3%	32.6%	18.4%	81.6%
Maui-5	2804	3075	271	40.31	3.2	20.3%	16.1%	17.6%	33.3%	66.7%
Maui-6	2785	3002	217	38.46	3.28	17.9%	17.5%	30.0%	31.8%	68.2%
Moki-1	2073	2410	337	22.38	7.8	21.8%	13.0%	32.7%	44.7%	55.3%
Average							21.3%	15.7%	28.2%	32.1%